Online Partial Discharge Measurement in a High Noise Environment

by

Nathan Dale Jacob

A Thesis Report

Submitted to the Faculty of Graduate Studies

in Partial Fulfillment of the Requirements

for the Degree of Masters of Science

Department of Electrical and Computer Engineering

University of Manitoba

Winnipeg, Manitoba, Canada

Acknowledgment

First I would like to thank my advisors Dr. Behzad Kordi, and Dr. David Swatek for their support and guidance through this thesis.

I extend thanks to Manitoba Hydro Research and Development for their financial support, and to the examining committee Dr. W. Ziomek, Dr. J. Paliwal, and Mr. W. McDermid for their evaluation of this work.

Lastly I would like to thank my colleagues, and many mentors in Manitoba Hydro's Insulation Engineering and Testing Department who have greatly contributed to my learning in the subject of high-voltage testing and electrical insulation diagnostics.

ABSTRACT

This thesis deals with the online measurement of partial discharge (PD) in a high-voltage direct current (HVDC) converter station. The HVDC station is a particularly challenging environment for PD measurement due to elevated interference levels caused from the switching of the thyristor-controlled converters.

Online PD measurements are performed on two specimens, one is an HVDC converter transformer and the other an HVDC converter wall bushing. The measurements are performed in the high-frequency range between 400-kHz to 30-MHz with a modern PD measurement instrument that employs a signal processing technique known as feature extraction.

The results demonstrate that online measurement of PD in an HVDC station environment is possible. Input filtering and feature extraction methods can mitigate the converter interference. The feature extraction methods can also isolate individual PD phenomena, and allow for the trending and monitoring of insulation degradation. Furthermore, specific strategies for PD measurement and analysis are developed.

TABLE OF CONTENTS

LIST OF FIGURES

1. INTRODUCTION

1.1 Overview

The fundamental purpose of electrical insulation in high-voltage apparatus is to sustain the high electric stresses within the apparatus in order to allow for the generation and transmission of electricity to end users, or customers. The integrity of electrical insulation in high-voltage (HV) apparatus is therefore essential for operation of the power grid. A phenomenon which can compromise the integrity of electrical insulation is known as partial discharge. Partial Discharge (PD) in electrical insulation is a phenomenon where applying high-voltage across an insulation system causes localized breakdown or arcing across small voids inside that system, or alternatively tracking across insulation surfaces. Over time, sustained PD activity will degrade the insulation level of the system and can cause eventual failure. Therefore the occurrence of PD in electrical insulation is an indication that the integrity of an insulating system has degraded.

Insulation degradation causing failure of electrical apparatus is undesirable for a number of reasons. One reason is due to the cost of repair and replacement

of the failed equipment. Often failures can be violent, resulting in an explosion where fragments of the apparatus are ejected with high velocity. These sort of failures have the potential for collateral damage to other apparatus located in a transmission station, and pose a safety risk for the employees working in the station. Insulation failures are also undesirable because the downed equipment reduces the revenue that may be generated from power sales, and affects the overall stability and reliability of the power transmission system.

For the mitigation of equipment insulation failures, the acquisition and interpretation of PD measurement data on HV apparatus becomes valuable. These measurements have the potential to identify insulation defects in the apparatus and enable the prevention of failures before they occur. The most common methods of PD measurement are performed electrically in the high-frequency range between 30-kHz and 500-kHz. When a PD occurs in an insulation, an electromagnetic pulse is produced that propagates away from the site of the insulation defect in all directions within the apparatus. The measurement of the PD pulse is performed with a circuit designed to couple the high-frequency currents induced from the electromagnetic pulse. However, in addition to the PD signal, there are other signals in this frequency range that can be induced in the PD measurement. These signals which are external to the apparatus act as electromagnetic interference, making the acquisition and interpretation of PD measurement data more complex.

Currently within the power utility industry, there are a variety of specialized electronic instruments designed for the purpose of measuring PD activity on HV apparatus while online. However, these apparatus are often located in transmission stations that have a congestion of other HV equipment, as well as overhead transmission lines. As a result, these stations inherently have high levels of electromagnetic interference, also referred to as noise. The noise which is external to the apparatus, may be from multiple sources, such as communications systems or radio stations, air-corona discharge, and PD occurring in neighboring apparatus. Additionally, some transmission stations containing power electronic devices such as high-voltage direct current converters, motor drives or static compensation, have elevated levels of electromagnetic interference due to the switching operations of the power electronic devices. Because of the way in which electrical methods of PD measurement are performed, environments with high electromagnetic interference make PD measurement difficult. The interference, or noise, appears in the PD measurement and hinders the ability to distinguish the interference from actual PD within the electrical insulation.

Recent developments in the area of digital signal processing have produced some modern PD measurement instruments that have noise separation capabilities that can filter out or identify some of the interference. These instruments use so-called feature extraction methods to distinguish and separate multiple PD phenomena from noise based on characteristics about the shapes of the pulse waveforms cap-

tured in measurement. However, these instruments are relatively new technologies so there has been little chance to confirm their effectiveness [1].

This thesis deals with electrical online measurement of PD performed on high voltage direct current (HVDC) apparatus located within an HVDC station. The HVDC station environment is a particularly challenging environment for the performance of online PD measurement due to elevated levels of electromagnetic interference caused by thyristor converter valve switching in the HVDC conversion process. There is also significant interference from external air-corona due to high electric stress at the surface of conductors and hardware which exceeds the corona inception level. The interfering corona can occur from either alternating current or direct current voltage sources.

The development of methods for online PD measurement are considered particularly valuable for the HVDC station application. Because of the large quantity of bulk power transmitted through these stations, failures are more detrimental to the power grid. Additionally it is the experience of the utility (Manitoba Hydro) that the failure rate of HVDC equipment is somewhat higher than for standard transmission stations and it is believed that PD measurement could potentially have found defects in the insulation system prior to some failures [2].

In this work, methods for online measurement, and subsequent analysis of PD data, are presented for two different types of HVDC apparatus. One is an oil filled HVDC converter power transformer, rated 262 MVA, with a 230kVac line-winding

and a 106kVac valve-winding, that is insulated for 375 kVdc. The other is a gas-filled HVDC converter wall bushing insulated for 500kVdc. A characterization of the noise environment present within the HVDC station is analyzed in detail. In addition, methods for noise identification and filtering are examined. For the oil-filled transformer specimen a series of measurements performed periodically over a three year period are analyzed with the aim of observing long term degradation of the insulation through trending.

1.2 Research Objectives

There are essentially two main goals for this research:

1. To characterize the nature of the electromagnetic interference present within the HVDC station environment, and determine what influence this interference has for the measurement of PDs on HVDC apparatus.

2. To determine the feasibility of online partial discharge measurement in the high noise, HVDC station environment and to determine whether this information may be used for the condition assessment of electrical apparatus.

1.3 Organization of the Thesis

This thesis is divided into six chapters as described below:

Chapter 1: Introduction of the project, giving an overview of the work done and identifying the goals for this research.

Chapter 2: Background information pertaining to the measurement of partial discharges. A brief discussion of partial discharge processes in electrical insulation is provided. Discussion extends to both traditional and modern methods for on-line PD measurement, and the associated challenges with online measurement in high noise station environments. A modern method for feature extraction of PD measurement data, which has been used in this research, is also presented.

Chapter 3: Discussion about the nature of the HVDC noise environment, and the nature of mixture of voltage stresses that are exerted upon HVDC equipment while in operation. It also discusses what impact the noise and mixed voltage stresses have for the online measurement and interpretation of PD on HVDC apparatus.

Chapter 4: Presentation of an online measurement method for PDs in an oil-paper insulated HVDC converter power transformer. An equivalent circuit model for the measurement method is proposed, and the measurement sensitivity of the method is analyzed. Data from actual online PD tests performed on the HVDC converter power transformer are presented and analyzed. The measurement data is post-processed with the aid of a feature extraction algorithm supplied by the manufacturer of the online monitoring test instrument.

Chapter 5: Presentation of an online PD measurement performed on a gas

insulated HVDC converter wall bushing which had a known insulation defect that was suspected of causing internal discharges. A comparative method of online PD measurement that was used to identify the presence of internal PD is presented.

Chapter 6: Conclusions about the findings from this research. A discussion about future work is also presented here.

2. BACKGROUND

2.1 Physical Processes Behind Partial Discharges in Electrical Insulation

Partial discharge (PD) in electrical insulation has been defined as a localized electrical discharge that only partially bridges the insulation between conductors and which may or may not occur adjacent to a conductor [3]. Partial discharges are caused when high voltage is applied to an insulation system in excess of the discharge inception voltage and may be as a consequence of localized concentrations of electric field stress at defects within the volume of the insulation, or on its surface. When the stress becomes sufficiently large, an electrical discharge, known as a partial discharge is produced. In the production of PD, energy is released, and may be observed in the form of an electrical pulse current. The energy may also manifest itself in the form of electromagnetic radiation, acoustical sound or chemical reactions within the insulation system.

Often, the site of an insulation defect causing PD is in the form of a void or inclusion within the volume of an insulating material. In an insulating system

where no void is present, the electric field stress from an applied voltage is graded uniformly from the high-voltage termination to the ground potential. This grading of stress is due to the permittivity inherent in the dielectric materials. However, where there is a defect in the form of a void within the insulating material, a distortion in the field produces a stress enhancement local to the void. This is because the void normally contains gases that have a dielectric constant that is lower than the surrounding insulating material.

In general, the most common forms of PD are caused from insulation defects having gas-filled voids in a solid or liquid dielectric material. As a result, the physics which govern the phenomena of PD occurrence within an insulation system are similar to the Townsend mechanisms for ionization and breakdown in gaseous dielectrics [4].

2.1.1 Townsend Mechanisms for Gas Discharge

The mechanisms by which partial discharges are produced in gas-filled voids within an insulation system can be described in part by the Townsend mechanisms for ionization and breakdown of gases under electric stress [4]. Under electric stress, ionization within a void is initiated when a free electron is accelerated in the direction of the applied field. When this electron collides with neutral molecules in its path, the bombardment liberates other electrons and produces other positively charged ions. These newly liberated electrons and ions go on to cause further

bombardments with other neutral molecules to liberate more, and more electrons. The multiplication of free electrons in the void produce what is referred to as an electron avalanche. The number of electrons, n, produced in the avalanche that will arrive at the positive polarity (anode) void wall, is defined by,

$$n = \frac{n_0 e^{\alpha d}}{1 - \gamma(e^{\alpha d} - 1)}, \tag{2.1}$$

where d is length of the void in the direction of the applied electric field. The parameter α is called Townsend's first ionization coefficient and is defined as the number of electrons produced per unit length of path traveled. The numerical value of α depends on the type of gas in the void. The parameter γ is called Townsend's second ionization coefficient and is defined as the number of electrons released from the cathode per incident positive ion. This coefficient relates to the liberation of electrons from neutral molecules caused by interactions with positive ions and photoelectric processes in the void. The parameter n_0 is the number of primary, or initiatory electrons, available at the negative polarity (cathode) void wall.

The avalanche can also be be defined in terms of current as,

$$I = I_0 \frac{n_0 e^{\alpha d}}{1 - \gamma(e^{\alpha d} - 1)}. \tag{2.2}$$

In (2.2), the parameter I_0 is analogous to the number of initiatory electrons

n_0 in (2.1). The avalanche current I increases exponentially as the denominator in (2.2) approaches zero. Therefore when conditions in the void satisfy (2.3), the current becomes very large and the gas in the void breaks down. The gases in the void become a conducting plasma.

$$\gamma(e^{\alpha d} - 1) = 1 \tag{2.3}$$

This condition satisfies the criteria for a Townsend type discharge and will produce a partial discharge within the void.

2.2 Equivalent Circuit for the Occurrence of Partial Discharge

In high-voltage literature the phenomena of PD in electrical insulation is commonly modeled by a simplified equivalent circuit as shown in Fig 2.1 [4–6]. In this equivalent circuit, a *Voltage Source* applies a voltage across an insulating material. The bulk portion of the insulation is modeled by a capacitance C_a with an internal resistance R_a. The capacitance C_a models the dielectric material, where the capacitance holding charge, effectively grades the voltage stress applied to the insulation. The resistance R_a represents internal leakages in the insulation. The resistance of of R_a is expected to be very large, in the order of giga-ohms. A defect having potential for producing PD is modeled with a capacitance C_c, a resistance R_c, and a *Spark Gap*. The *Spark Gap* will discharge when the electric

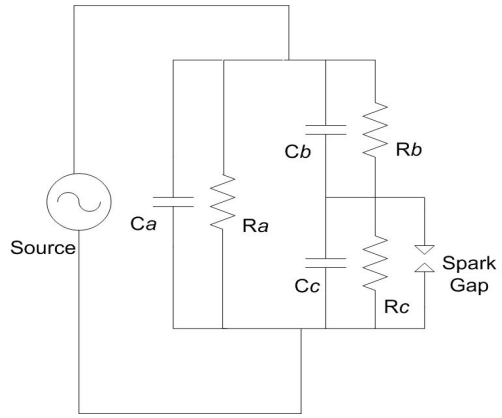

Fig. 2.1: Equivalent circuit representation of PD occurring within a void in an insulating material under electric stress.

stress across defect becomes sufficiently large. This models the occurrence of a PD. In the vicinity of the void there exists the surrounding dielectric between the void and the *Voltage Source* electrodes. The surrounding dielectric is modeled as a capacitance C_b and a resistance R_b, which are the capacitance of the dielectric material and the leakage respectively.

The equivalent circuit model is often used as a tool to aid in the understanding of PD occurrence, and to emulate the behavior PD activity in electrical insulation [7]. In this model, a partial discharge current pulse is observed across the terminals of the insulation when the *Spark Gap* breaks down. At this moment the void capacitance discharges into the gap and the impedance across the terminals of the insulation changes suddenly, which causes a PD pulse current. Although this model adequately emulates the occurrence of PD, in reality the generation of a PD pulse current at the terminals of the insulation is caused from an electromag-

netic pulse which propagates through the insulation and induces a current pulse at the terminals of the specimen. There are no a sudden changes to the capacitive impedance at the terminals of the specimen as a result of the PD [8]. It has been observed in laboratory measurements that there is no change in the capacitance at the terminals of an insulation when a PD occurs internally [7]. However, equivalent circuits are still used to simulate of PD activity for the development of PD measurement instruments.

2.3 Electric Stress and the Recurrence of Partial Discharges

The recurrence of PD in an insulating material is dependent upon the type of electric stress which is applied to the material. If the magnitude of the electric stress is sufficient to cause the inception of PD within voids in the insulating material (i.e. satisfying (2.3)), the recurrence of these discharges is dependent upon whether the applied electric stress is from a direct or alternating voltage source.

2.3.1 Recurrence of PD Under Direct (dc) Voltage Stress

Assume that an increasing (ramp) direct voltage is applied to a slab of dielectric material with a single void as shown in Fig. 2.2. When the direct voltage becomes sufficiently large, a PD occurs. After the initial occurrence of the PD breakdown within the void, positive and negative ions remain behind and collect near the void

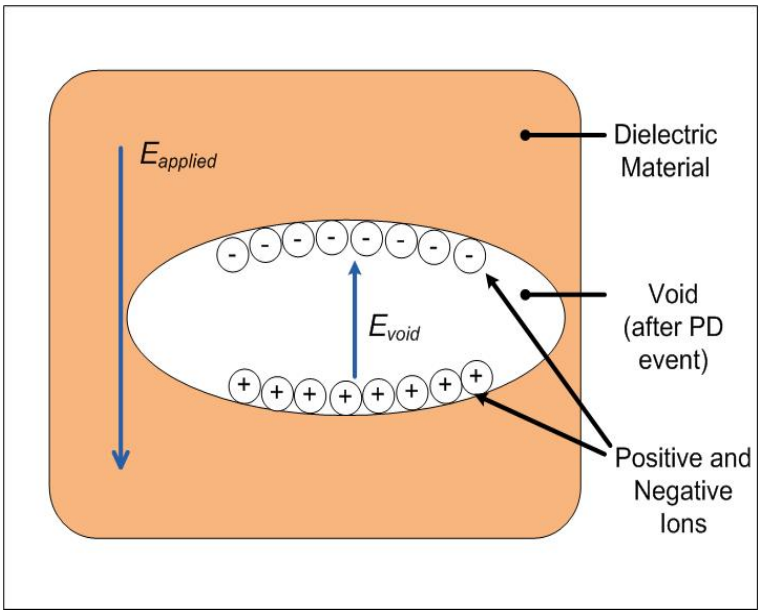

Fig. 2.2: Positive and negative ions suspended in a void after a PD event. Reducing field stress within the void.

walls. These ions form dipoles across the void which orientate themselves opposite to that of the applied electric field. This has the effect of reducing the field stress and voltage across the void [4].

If the applied direct voltage continues to rise after the initial discharge, PDs will occur each time the void voltage meets the breakdown criterion given in (2.3). However, if the applied direct voltage stops and holds at a constant value, and the dipoles, or ions formed from the preceding discharge activity remain behind, they will maintain a reduced field in the void and thus no further discharge activity will occur. Referring again to equivalent circuit in Fig. 2.1, when a direct voltage is applied for the *Source*, the system reaches a steady state when the capacitive elements are fully charged. At this point the voltage across the void will be governed

by only the insulation resistive elements, given by,

$$V_c = \frac{R_c}{R_b + R_c} V_{Source}. \tag{2.4}$$

At steady state, the void voltage V_c should in theory remain below the breakdown level given by (2.3) and discharge activity in the void should cease. However, in some insulation systems under direct voltage stress, the recurrence of can be caused from internal leakages within the insulation system and chemical processes within the void. Depending upon the material of dielectric surrounding the void, the ions forming the dipoles can lose their charge by reacting with the void walls. This chemical process is called diffusion [4]. As the ions within the void diffuse and become neutral, the electric field stress within the void will again increase until satisfying the conditions for discharge in (2.3). The rate of diffusion is dependent upon a variety of factors including the energy of the initial discharge, type dielectric material, dimensions of the void, temperature, and pressure. The rate of diffusion will also dictate the repetition rate of PD in the void under direct voltage stress. The process described may be more typical of a cast epoxy type insulation system.

In the recurrence of PD under direct voltage stress, after discharge has extinguished in the void, the void recovers and diffusion processes begin to occur. As a result the voltage across the void increases at a rate dependent upon the dielectric material's internal capacitances and leakages. This rate of increase is defined by a

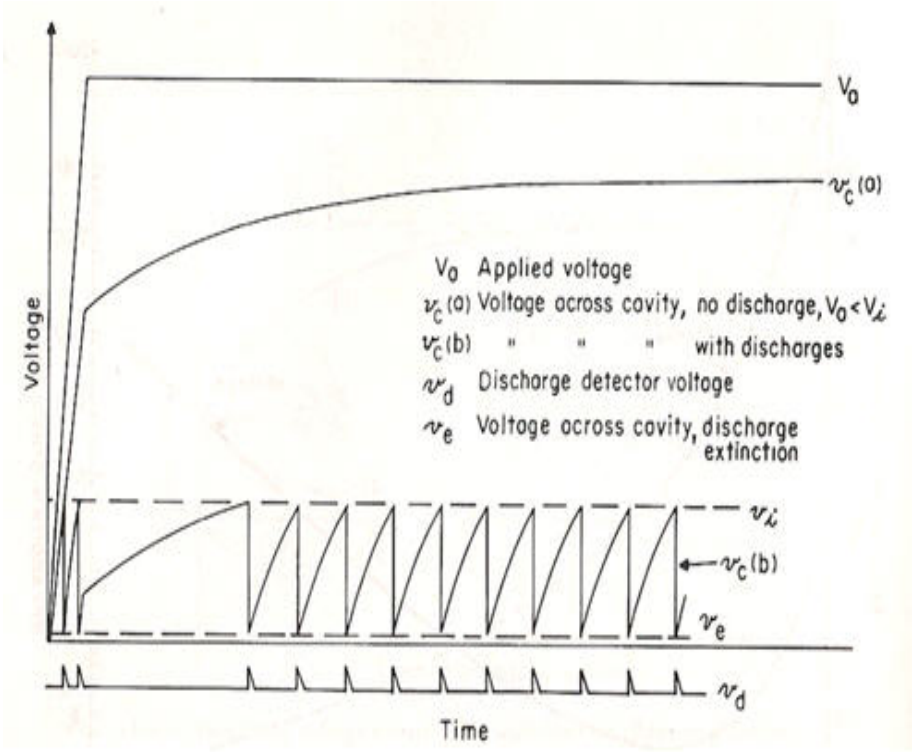

Fig. 2.3: Suggested PD Pattern for a dielectric void under direct voltage stress , adopted from [6].

time constant τ, obtained from [6], and is given by,

$$\tau = \frac{R_b.R_c}{R_b + R_c}(C_b + C_c). \tag{2.5}$$

Therefore the repetition rate of PD is given by,

$$f = \frac{1}{\tau}. \tag{2.6}$$

The recurrent discharge pattern for an insulation system under direct voltage will be similar to that shown in Fig. 2.3, obtained from [6]

If the PD is highly repetitious then the insulating material may degrade to failure more quickly. However, diffusion is normally a relatively slow process in many dielectric materials and under direct voltage stress the repetition rate of PD is low. Normally PD activity caused from direct voltage stress is several orders of magnitude lower than PD activity caused from alternating (ac) voltage stress [6].

2.3.2 Recurrence of PD Under Alternating (ac) Voltage Stress

Under alternating voltage stress, recurrence of PD is higher than for direct voltage. The recurrence is caused by the regular polarity reversals for the applied electric field of the alternating 60-Hz sinusoid voltage waveform. Once the magnitude of the alternating voltage is sufficiently large to satisfy the conditions for discharge as in (2.3), PD inception happens and a discharge occurs. Similar to the direct voltage case, after this initial discharge, ions form dipoles spanning the void walls. In the direct voltage case these dipoles along the void walls acted to extinguish the PD activity and slowed recurrence. For alternating voltage stress, as soon the polarity of the applied electric field reverses with the sinusoid, the ions in the void will enhance the field stress and encourage the recurrence of discharge. This phenomena makes PD much more repetitious under alternating voltage stress. The ionization within the void often makes the extinguish level of the PD activity lower than the inception level. Therefore once the voltage has been raised sufficiently high to incept PD, it will have to be reduced to a value lower than the inception

voltage in order for the PD to extinguish, and diffuse the ionization.

In some cases, after inception it is possible for the discharges to extinguish themselves at a fixed alternating voltage. A variety of phenomena can cause the discharges to extinguish. One possibility is that gross ionization within the void can saturate the void, where ions line the walls of the void and make it conductive. This reduces the voltage across the void and the PD is extinguished. Similarly, it is also possible for chemical reactants from the discharges to line the inner walls of the voids. Lastly, increases in pressure in the void after recurrent discharges can also extinguish the PD.

2.3.3 Recurrence of PD Under Transient Switching Voltage Stress and Harmonics

Switching transients caused from power electronic devices can have an influence on PD in electrical insulation. The deleterious effects of PD caused by variable frequency drives are well documented on random wound induction motors [9]. These drives are composed of insulated gate bipolar-transistors (IGBTs) which control the motor speed and torque. The switching transients and harmonics produced as a result of IGBT switching in the voltage source conversion process are graded differently by the motor insulation than the regular 60-Hz, power frequency voltage. Often these harmonics produce high stress regions in motor winding insulation system closer to the winding terminals, and the source of the harmonics.

The regions of higher stress are therefore more susceptible to PD, and premature insulation failure.

Similarly to IGBT controlled motor drives, thyristor controlled HVDC valve converters produce fast switching transients and harmonics in the AC to DC conversion process. Equipment connected to a HVDC converter valve group, may be subjected to high stress regions within their insulation due to the production of transients and harmonics. PD caused from an HVDC converter are likely to be recurrent with the thyristor firing.

2.4 Partial Discharge Degradation and Failure Mechanisms

Failure of electrical apparatus by PD is often classified by what is called an erosion process [4]. Recurrent discharges within a void will cause the void to grow. This growth can be caused by the impact of electrons and ions on the void walls which break molecular bonds in the surrounding dielectric. In some cases, it is also possible that chemical reactions, triggered by PD within the void, are corrosive to the surrounding dielectric. As erosion occurs, it causes PD to move to different regions within the insulation system. Once the erosion has grown to a certain point the electrical insulation may be so severely compromised that the risk for a complete electrical failure increases.

In organic insulating systems such as oil-paper insulated apparatus, the degradation of PD often manifests itself in the form of what is called tracking. Tracking

is the formation of a conductive path, caused by carbon deposited along an insulation surface [4]. Within a power transformer this may be between layers of the winding paper insulation, or along the surface of the winding press-board material, or at interfaces such as the oil end of bushings. The presence of PD causes degradation of the insulating paper and thus carbon is deposited on the paper surface. Similar to erosion, tracking may cause the site of the PD to move to another region of the insulation system. Because the carbon track is conductive, it can severely compromise the insulation and increase the risk for failure of the apparatus.

2.5 Methods of Online Measurement of Partial Discharges

The two most common forms of online PD measurement used in industry include acoustical and electrical measurement techniques [10]. As mentioned in Chapter 1, this thesis focuses on electrical methods of online measurement performed in the high-frequency range. For any electrical method of PD measurement, it is not possible to measure the actual PD pulse current which occurs at the site of the insulation defect. This is because it is not practical to install sensors within the bulk insulation system. In addition, it is not possible to cover all regions of the insulation in which PD may occur. Instead, the measurements are carried out by a method of coupling into the insulation. The electrical coupling monitors the artifacts of electromagnetic waves that are emitted by the PD.

One common form of a coupling involves the use of a coupling capacitor. Ca-

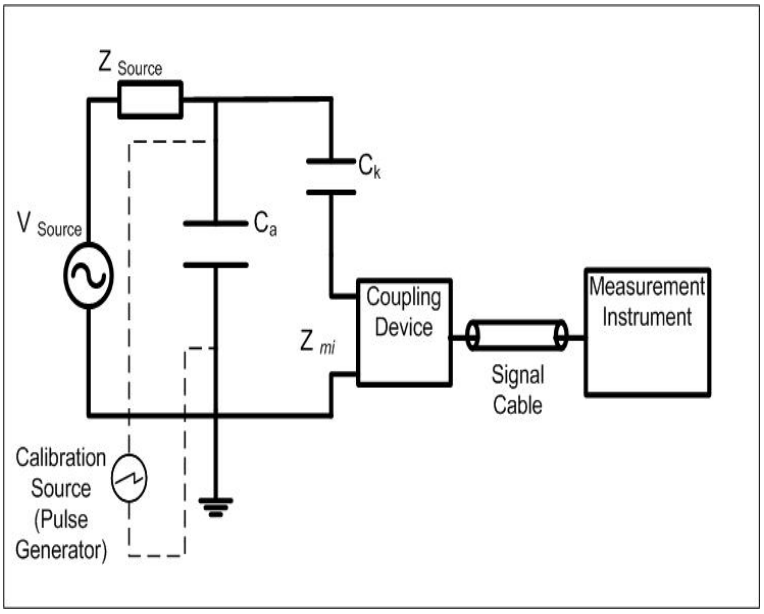

Fig. 2.4: Basic Partial Discharge measurement circuit.

pacitive coupling essentially utilizes a high-voltage capacitor to couple into the insulation system while under voltage stress. The capacitor may be a part of the apparatus, such as the capacitance tap on a HV bushing, or it may be an entirely separate high-voltage capacitor connected in parallel with the equipment being monitored under test. A schematic of a basic capacitive coupled PD measurement circuit is shown in Fig. 2.4.

In Fig. 2.4, the source V_{Source} has a source impedance Z_{Source}. The specimen under test is denoted C_a, and the high-voltage coupling capacitor is C_k. When a PD occurs in the specimen C_a, the coupling capacitor supplies a displacement current to compensate for the PD current in the specimen. The current is displaced across a measuring impedance in the **Coupling Device**. The **Coupling Device**

often functions to provide the **Measurement Instrument** isolation from voltage spikes that may damage the instrument, and to condition the signal prior to measurement. Some examples of a **Coupling Device** can include elements such as a ground isolation transformer, a high-pass filter and/or a fiber optic converter. With the PD signal conditioned, the acquisition is transmitted to the **Measurement Instrument**.

A potential source of error in the measurement is present if there exists large stray capacitances in the measurement circuit. A large stray capacitance to ground present near the specimen C_a can influence the sensitivity of the measurement. When the PD occurs, stray capacitance can supply part of the displacement current to the PD which therefore does not appear the measurement. In order to have good sensitivity for PD measurement the coupling capacitance C_k must be orders of magnitude larger than any stray capacitances.

Another factor to the sensitivity of the measurement, is that the current displaced at the terminals of the specimen is not equal to the PD pulse current at the site of the defect. This is because the displacement pulse current observed in measurement is an induced current caused from an electromagnetic wave that propagates from the defect. This wave propagates through the insulation before reaching the terminals of the specimen C_a. In the case of inductive equipment there is also a transmitted pulse that follows the winding to the terminals. Losses in the dielectric and shunt capacitance to ground may act to attenuate the pulse-wave

before arriving to the point of measurement. Therefore if two defects with equal PD magnitudes are located at different distances from the point of measurement, the measured displacement currents will not be equal. The defect which is located closer to the point of measurement (or terminals of the specimen C_a) will appear to produce larger PD pulses than the defect located deeper within the bulk of the insulation. This is significant because it determines that the measured magnitudes of PDs are not sufficient to establish how damaging they may be for the insulation. Very small pulses may indicate a serious problem deep in the insulation, and alternatively seemingly large pulses occurring near the point of measurement may not be so severe. In the case of inductive equipment, fast rise time pulses of short duration often originate near the measurement terminal while ringing pulses have been transmitted through the winding.

Because of these problems associated with measurement sensitivity, no significant knowledge about the severity of PD may be determined based solely on the magnitude of the pulses acquired during online PD measurement. Therefore if PD measurements are to be used in the diagnosis of HV apparatus, the measurements must be trended over time. If changes in the magnitude, or repetition rate of PD pulses are observed over time, at a variety of operating and seasonal conditions, then this may indicate a degradation in the integrity of the insulation.

2.5.1 Quantification of Partial Discharge Measurement

The PD pulse displacement current occurring at the coupling capacitor C_k, appears as a simple pulse in millivolts (or milliamperes) at the terminals of the measuring instrument. From this signal some basic metrics are formed in an attempt to quantify the severity of the discharges, and determine what risk they have for failure of the equipment.

The most simple metric which may be measured relates to the size, or peak magnitude of the measured discharge in millivolts. This maximum is often denoted as $Qmax$. However, $Qmax$ for reasons relating to measurement sensitivity can be misinterpreted if the measurement is performed with the assumption that the pulse magnitudes acquired are equal to, or are directly proportional to the PDs occurring at the site of the insulation defects. For online measurements, the parameter $Qmax$ should only be used as a relative comparison for trending the PD activity observed over time.

Another basic quantitative metric for PD is the repetition rate of the PD activity. Repetition rate under alternating voltage is measured in pulses-per-second (pps). Repetition rate under direct voltage during factory tests on converter transformers is typically measured over a 30 minute period. Repetition rate is a useful quantity for trending over time because it is expected that as an insulation becomes degraded due to PD, the repetition rate of the PD can increase. Degrading processes such as spark erosion and tracking may lead to the spread of PD to other

discharge sites. Therefore it is expected that with degradation, the overall number of discharges will increase.

One parameter very commonly used to quantify the magnitude of PD pulses is called the apparent charge of the PD [3]. For a PD test performed with measurement of apparent charge, the system as shown in Fig. 2.4 must first be calibrated with the use of a calibrator injection source, prior to measurement. The calibrator source produces current pulses that have similar characteristics to those of PD. The rise-time of the pulses are on the order of a few nanoseconds, and the overall duration less than a micro-second. The injection source produces pulses with a known quantity of charge (in pico-Coulombs). The charge is injected across the terminals of the test specimen C_a. The measurement setup is then calibrated such that the magnitude of the voltage pulse which appears across the measuring impedance is scaled to the value in pico-Coulombs that was injected across the specimen C_a. After calibration, and the voltage source is applied to the insulation, measurement of PD is performed with the data recorded in apparent charge. Like the quantity $Qmax$, the measured apparent charge of a PD pulse is not equivalent to the actual charge displaced at the site of the PD for the same reasons as mentioned earlier.

2.5.2 Phase Resolved PD Measurements for Alternating Voltage Stress

Phase resolved PD measurement under alternating voltage stress is one of the earliest genres of pattern recognition in PD measurement. In a phase resolved

PD measurement, the magnitudes of individual PD pulses are plotted relative to their phase location on the 60-Hz sinusoid waveform. This yields a phase resolved PD pattern. If the phase resolved measurement produces a pattern, the pattern may be used to identify the type of insulation defect causing PD. Identification is valuable because the information can be used to plan maintenance and whether to repair, replace, or continue to monitor the equipment. This information can contribute to the prevention of insulation failures.

For a pure alternating voltage stress applied to an insulation system the phase resolved PD pattern found in measurement should be repetitive over the 60-Hz interval, meaning it should respond the voltage stress applied. If the discharge pattern is entirely random over the 60-Hz interval it may be characterized as external noise. There should also be some degree of statistical variation in the phase location of the PD pulses with each voltage cycle. PD is a stochastic process, which is dependent on the availability of an initiatory electron to produce the electron avalanche. This electron is not likely to be available at the exact same instant in time with respect to phase location of each recurrent cycle of the sine wave. This causes slight variations in the phase location of the PD pulses. Pulses that do appear in the exact same phase location cycle to cycle are often caused by external noise. For example power electronic devices would produce electromagnetic pulses in the measurement which occur at exactly the same phase location at every cycle.

For an alternating sinusoid the phase resolved PD measurement pattern is

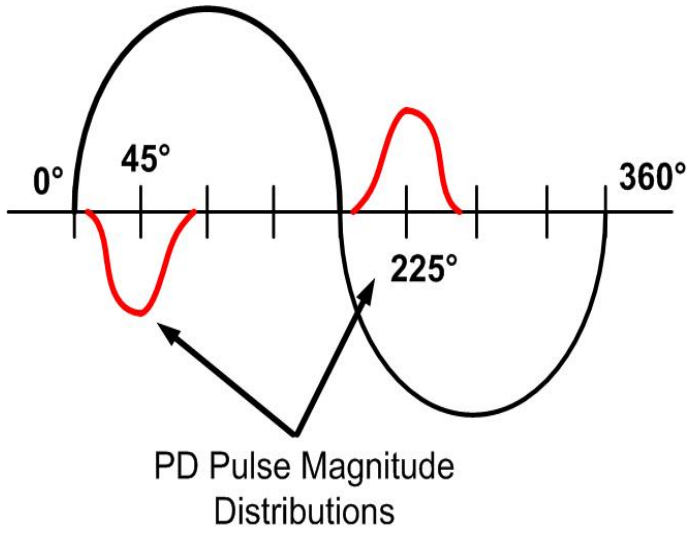

Fig. 2.5: Gaussian (Weibull) distributions of PD pulse magnitudes in response to alternating voltage stress.

expected to produce a Weibull (extreme value) or Gaussian (normal) distribution of pulse magnitudes relative to phase-angle [11–13]. For a defect such as a void in dielectric material, two symmetrical distributions of pulses located on the positive and negative half cycles are expected. The expected distributions for the PD pulse magnitudes are roughly as shown in Fig. 2.5.

The distributions of PD pulses respond to areas of increasing voltage magnitude on the sinusoid. The distributions are usually centered around the 45 and 225-degree phase angle locations and the polarity opposite to that of the voltage stress. In Fig. 2.5, the distributions are Gaussian (or Normal) distributed, however it is also common for the discharge patterns to be skewed, forming a Weibull type distribution. The pattern in Fig. 2.5 may be referred to as symmetrical, in that the positive and negative half cycles are mirror images of each other. It is

common for some insulation defects to have PD measurement patterns that are not symmetrical.

The most traditional methods of phase-resolved PD measurement utilize an elliptical time base on which PD pulse magnitudes are superimposed. Angular locations on the ellipse correlate with the phase locations of the actual voltage waveform stressing the insulation. The PD pulse magnitudes are shown on the ellipse at the location they occur with respect to the voltage waveform. Examples of some common phase resolved PD patterns are taken from [14] and shown in Fig. 2.6.

As was already mentioned, the purpose of producing a phase-resolved PD pattern is for the identification of a defect causing discharge. Engineers and technicians performing the tests look for patterns on the ellipse such as those shown in Fig. 2.6. In the figure the positive and negative peaks of the voltage stressing the insulation is represented by the (+) and (-) symbols respectively. The zero crossings of the sinusoid would dissect the ellipse perpendicular to the intersection between the (+) and (-) half cycles. The ellipse direction is clockwise. The zero degree mark is located on the left side of the circumference, and travels clockwise. The positive peak of the sinusoid at (+) correlates to the phase angle of 90-degrees. The negative peak of the sinusoid at (-) correlates to the phase angle of 270 degrees.

The phase-resolved PD patterns are documented for a variety of insulation

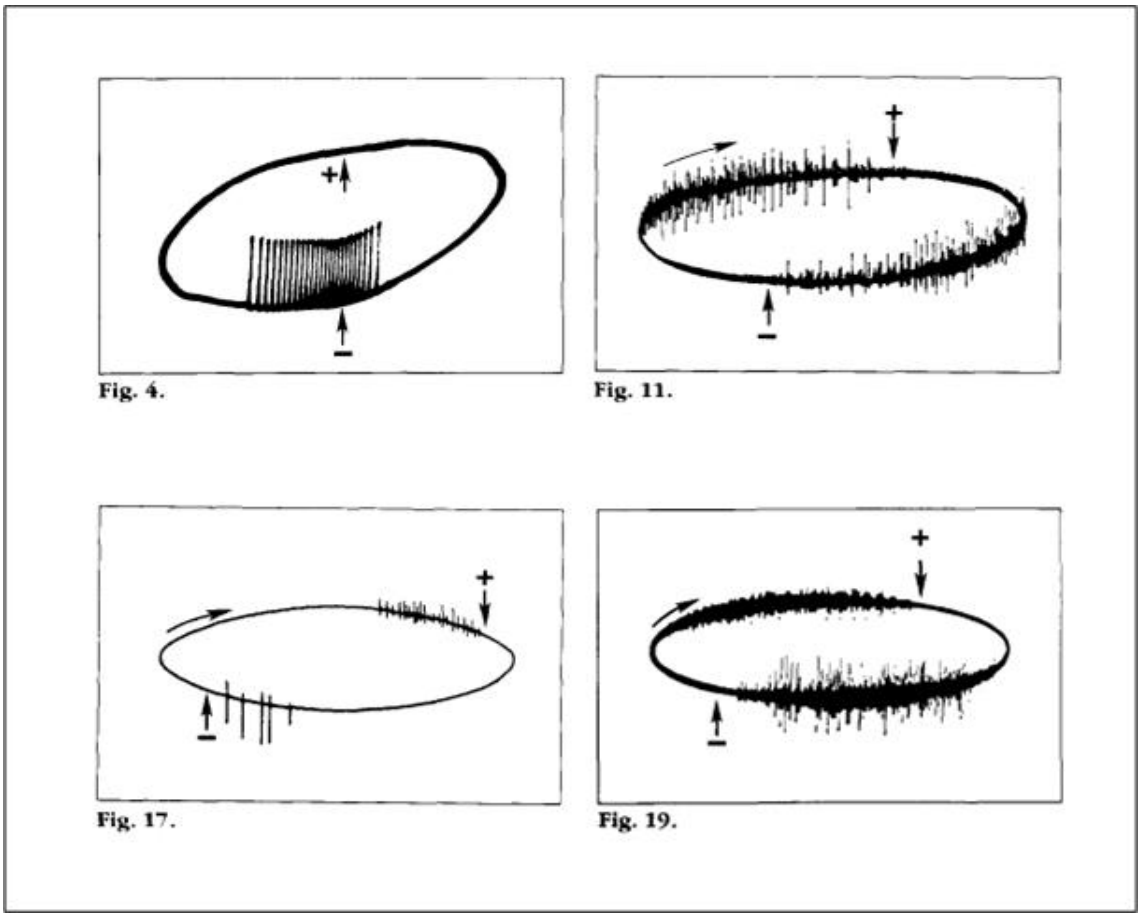

Fig. 2.6: Ellipse phase-resolved PD measurement patterns adopted from [14]

systems. In [14], some common patterns are given. These patterns were produced in laboratory tests where PD measurements are performed on specimens with known defect types. For example, Fig. 2.6 shows four known ellipse phase-resolved PD patterns. The upper-left quadrant shows an ellipse pattern from PD produced by a sharp protrusion in air. This sort of PD is commonly referred to as corona. The upper-right quadrant shows PD produced within voids in solid insulation. This type of defect is expected to produce a symmetrical phase-resolved PD pattern because the boundaries of the defect are made of the same dielectric material. In contrast to the PD pattern for a void within the dielectric material, the bottom-left shows PD at a void at the interface between the HV conductor improperly adhered insulation. This PD pattern is asymmetrical. Finally, the bottom right shows PD tracking along the surface of dielectric material. Patterns generated in these sort laboratory tests can be used to identify defects in measurements performed on actual apparatus.

Modern PD measurement devices also implement phase-resolved PD patterns for the identification of insulation defects. However, rather than an ellipse, many modern instruments plot the phase locations of PD pulse magnitudes relative to a sinusoid. In Fig. 2.7, a phase-resolved PD pattern is shown for discharges occurring in gas-filled voids within an oil-paper insulated instrument transformer. This pattern resembles the expected Gaussian distribution shown in Fig. 2.5.

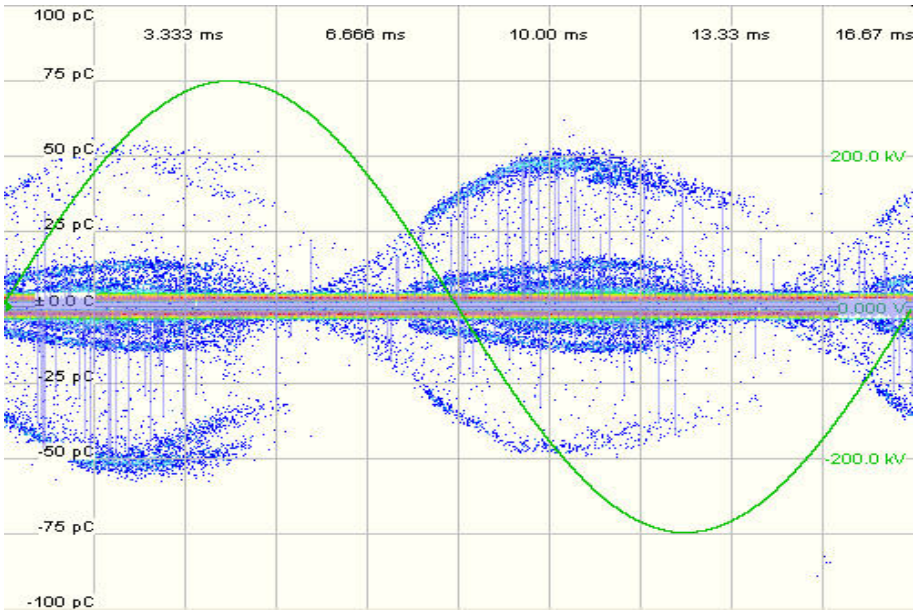

Fig. 2.7: Phase resolved PD measurement acquired from offline measurement of a 230kV insturment transformer

2.5.3 Measurement of PD Under Direct Voltage Stress

As mentioned in section 2.3.1, PD under direct voltage stress is recurrent due to leakages in the dielectric, and chemical processes of diffusion. The method of measurement for PD at direct voltage is essentially the same as for alternating voltage stress and the measurement circuit will be similar to that shown in Fig 2.4. However, because diffusion is a very slow process, the repetition rate of PD under direct voltage is very low. Because of this, online measurement of PD at direct voltage is often performed over much longer acquisition durations, as much as 30-60 minutes [15].

The main differences from PD measurement at alternating voltages, is that di-

rect voltage PD measurement cannot be analyzed relative to an alternating waveform. Therefore producing a phase-resolved PD pattern that may be analyzed for the identification of a defect is not possible. This makes identification of defects under direct voltage stress more difficult for dc insulation.

In some cases, the identification of noise is possible for direct voltage PD measurement. This is because the discharges that occur in response to direct voltage stress must be in the opposite polarity of the voltage applied. This information can be used to identify external noise, because wherever discharges with same polarity as the source are measured they can be ignored as external noise.

For the identification of PD at direct voltage there are essentially only two parameters that are available for analysis. The magnitude of the discharge q_i, and the time between discharges Δt_i. These quantities are measured as shown in Fig. 2.8.

From q_i and Δt_i, some methods in industry have been developed for generating patterns from the data that can be used to identify some simple defects in insulation systems. These patterns are called *Predecessor/Successor* diagrams [15, 16]. If a PD of a given magnitude occurs, a *Predecessor/Successor* diagram records the average time between the preceding discharge of similar magnitude and the succeeding discharge of similar magnitude. Values for these times between discharges are plotted on a graph for interpretation. From these, some simple types insulation defects producing PD are identifiable. However, these techniques are

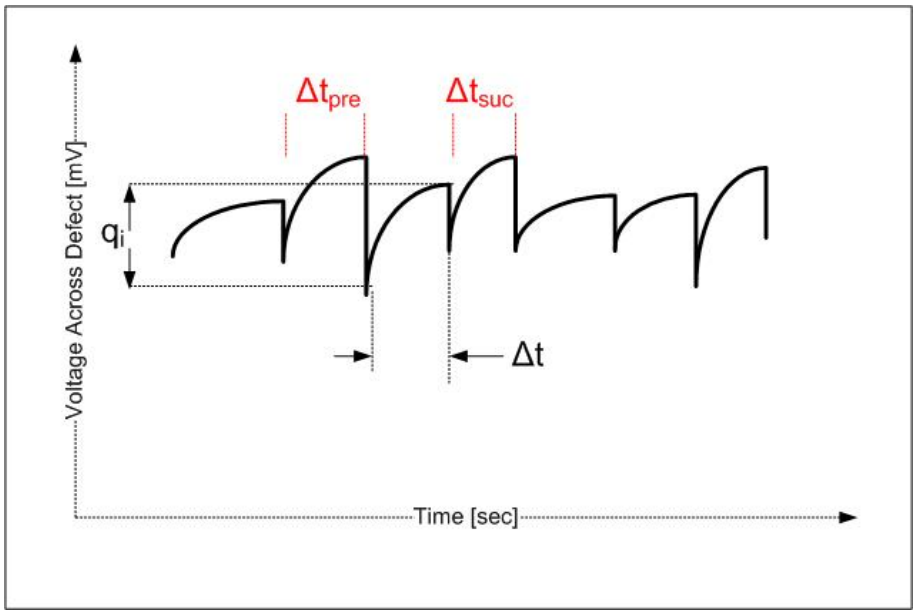

Fig. 2.8: Quantitative metrics for direct voltage pd measurement, q_i and Δt_i

only suitable when there is only one type of insulation defect producing discharges, when there are many multiple sources it becomes difficult to separate the phenomena and analyze.

These techniques are not used in the analysis of PD data obtained in this research. This is because for the HVDC equipment that PD measurements were performed on, the voltage stressing the insulation systems was not purely dc. The voltage stresses are mixed with direct, alternating and transient voltage stresses. Therefore analysis by *Predecessor/Successor* PD patterns is unsuitable for the data acquired, but is common during factory tests on converter transformers.

2.5.4 Influence of Noise in PD Measurement

The influence of noise in PD measurement will be elaborated on in Chapter 3. All that is necessary to say here is that noise in PD measurement can come from multiple sources. For electrical methods of PD measurement noise appears in measurement due to electromagnetic interference which is radiated or conducted from a noise source. Possible noise sources include external ac or dc air-corona, switching noise from power electronic devices, and PD that is occurring on neighboring equipment. To obtain good information in PD measurement, it is important to filter noise. This can be done during the measurement by analog filtering at the input of the measuring device, and/or by removing the noise digitally after measurement, through digital signal processing methods.

2.5.5 Feature Extraction Algorithms Used in PD Measurement

Some modern methods of online monitoring for PD have attempted to use signal-processing techniques to extract features about the PD pulse shape [17, 18]. The purpose of feature extraction for online PD measurement is that it can be used to separate external noise and corona from the measurement, as well as separate multiple sources of discharges occurring in the equipment. It was mentioned in section 2.5 that practical PD measurements are fundamentally required to be a trended measurement due to issues with measurement sensitivity. If multiple sources of PD are present in an apparatus, then these multiple sources can make the isolation of

defects and trending of their PD data difficult. By separation, it becomes possible to monitor and trend sources of discharge individually.

A popular feature extraction algorithm that has displayed some success for on-line PD measurements is known as the method of moments algorithm [16, 18]. For the acquisition of PD data in this thesis, the feature extraction is handled by the PD measurement instrument which is equipped with signal processing software to perform the algorithm. The instrument is called the PDBase and is manufactured by a company called Techimp Systems.

The purpose of the feature extraction is to capture information about the shape of an individual PD pulse. The theory behind this method is that PD pulses and electromagnetic interference pulses will have their own distinct waveform shape. If the shapes of the individual waveforms could be acquired and compared then it would be possible to separate the multiples sources of PD from the each other and the external noise. However, if a measurement instrument were required to record and store the individual time domain waveforms of each PD pulse current, this would require an exhaustive amount of computing power and memory. The method of moments feature extraction algorithm provides a dimensionality reduction of the time domain information.

In the method of moments algorithm, a discharge signal $s(t_i)$ is acquired by analog-to-digital conversion in K samples. A time-barycentre t_0, also called the time-position of the PD signal is computed by,

$$t_0 = \frac{\sum_{i=0}^{K} t_i.s^2(t_i)}{\sum_{i=0}^{K} s^2(t_i)}. \tag{2.7}$$

The Fast Fourier Transform of the signal $s(t_i)$ is $X(f_i)$ which gives the equivalent time length (T) and equivalent bandwidth (W) defined in (2.8 and 2.9),

$$T^2 = \frac{\sum_{i=0}^{K} (t_i - t_0)^2.s^2(t_i)}{\sum_{i=0}^{K} s^2(t_i)}, \tag{2.8}$$

$$W^2 = \frac{\sum_{i=0}^{K} f_i^2.|X(f_i)|^2}{\sum_{i=0}^{K} |X(f_i)|^2}. \tag{2.9}$$

Both equivalent time-length (T) and the equivalent bandwidth (W) are normalized quantities. These quantities are plotted on a feature extraction map, also referred to as a TW-Plane. On the feature extraction map the equivalent time length (T) measured in nanoseconds is plotted on the vertical axis, and equivalent bandwidth (W) measured in MHz is plotted on the horizontal axis. An example of the Feature Extraction Map is shown in Fig. 2.8.

In an online measurement, mapping to this two-dimensional space allows for the separation of multiple PD phenomena. Through separation, the ability to trend and monitor the individual defects causing PD is improved. For example, if a single defect producing PDs produces pulses of a specific shape, these pulses

are in theory, mapped to a specific location on the TW-Plane. During an online measurement, the transformation and mapping of PD pulse information to the TW Plane produces clusters of pulse data. Slow, long duration PD pulse waveforms will have larger equivalent time-length but smaller equivalent bandwidth. Conversely, fast, short duration PD pulse waveforms will have larger equivalent bandwidth and smaller equivalent time-length.

Isolation of the PD pulses produced by a single defect allows the operator to trend the discharge magnitude and/or the repetition rate of the PD over time. Once isolated, clusters of PD pulses can be analyzed by phase-resolved methods, or another method with the aim of identification of the defect causing discharge. In this thesis, the assignment and separation of cluster data was perfomed visually by the operator. However, artificial neural networks offer the possibility of future continuous online PD monitors where the assignment of clusters is handled by a computer [19].

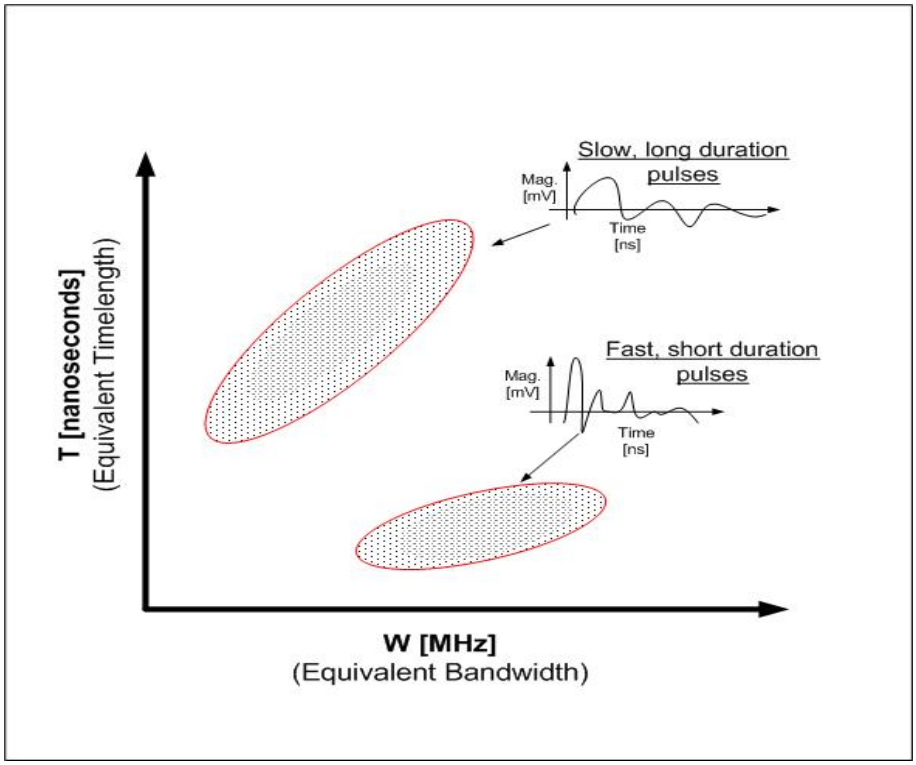

Fig. 2.9: Feature Extraction map displaying clusters of PD pulses transformed and mapped to the TW-plane.

3. CHARACTERIZATION OF HVDC VOLTAGE STRESSES AND THE HVDC STATION NOISE ENVIRONMENT

As mentioned in Chapter 1, the HVDC station environment presents many challenges for performing online PD measurements. These challenges are mainly due to difficulties associated with the mixed voltage stresses that are exerted on the equipment and the high levels of electromagnetic interference (noise) which is present within the HVDC station environment. This chapter describes the arrangement of equipment within the HVDC station, characterizes the mixture of voltage stresses exerted on the equipment, and analyzes the interference the HVDC station causes in online PD measurements.

3.1 General Arrangement of Equipment within an HVDC station

The PD data acquired and analyzed as part of this thesis were obtained at two different converter stations on Manitoba Hydro's two HVDC bipoles. The rectifier ends of the bipoles are located in northern Manitoba, where a majority of the electrical power generation is located, and the inverter end in the south, where a

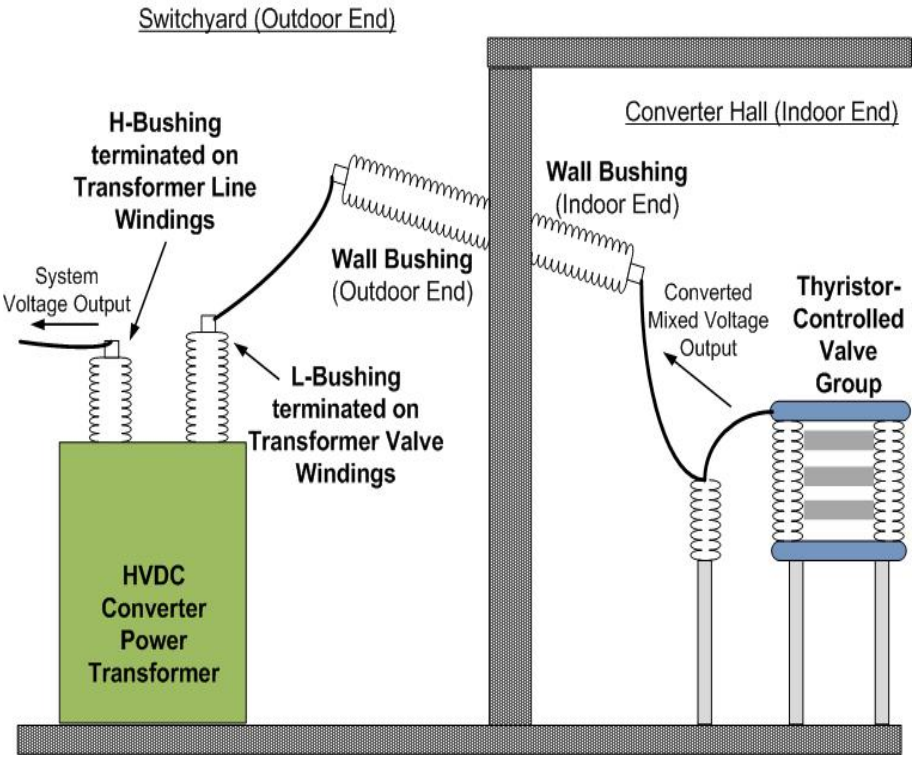

Fig. 3.1: Schematic of general arrangement of HVDC station equipment.

majority of customer demand is located and where major export tie lines originate. The arrangement of the HVDC equipment in this study is the same for both rectifier and inverter station ends of the HVDC link. A general arrangement of HVDC apparatus is shown Fig. 3.1.

In Fig. 3.1, an HVDC converter bridge is shown located within a building labeled as a thyristor controlled valve group. The inverter takes direct voltage transmitted by the HVDC link and converts it into an alternating voltage waveform. The converter bridge must be located indoors, because the equipment has to be installed in an environment where the temperature and humidity are controlled.

The converted alternating voltage waveform is then transmitted outdoors through a wall-bushing. The voltage transmitted through the bushing has a direct voltage component, an alternating voltage component, and a switching transient component. The voltage stresses leaving the converter bridge are therefore described as mixed. The mixed voltage exiting the wall bushing then enters the valve-windings of a converter power transformer. The alternating voltage component is stepped up to a transmission voltage level and the direct voltage component is removed through the valve-winding to line-winding transformation. Any harmonics not removed by the transformer's inductance are removed down the line by station filters, as well as large salient pole synchronous machines operating on the same bus.

In this thesis, online PD measurements are performed to the HVDC wall-bushing and both valve and line-windings of the HVDC converter power transformer.

3.2 Characterization of the Voltage Stresses on HVDC Apparatus

In the general arrangement shown in Fig. 3.1, the mixed voltage waveform produced by the converter valve stresses the insulation of the wall bushing, the valve-winding, and the valve-winding bushing. A simulation of Manitoba Hydro's HVDC system in operation, was performed in PSCAD software to observe the mixed voltage waveform. The simulated mixed, line-to-ground voltage stress is shown in Fig.

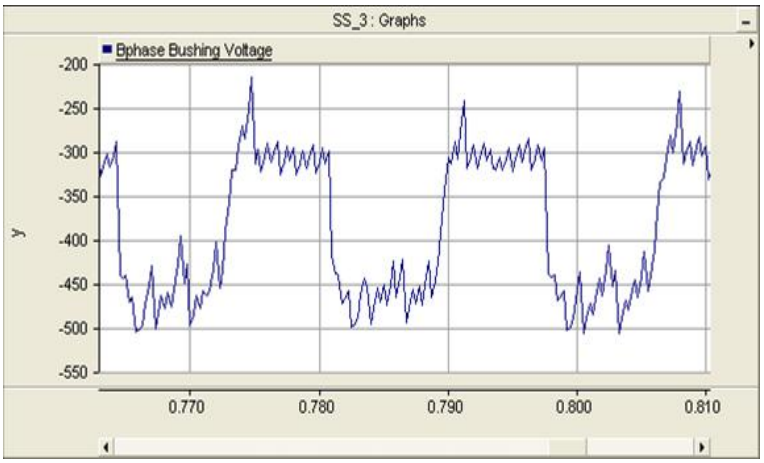

Fig. 3.2: Voltage waveform for line-to-ground mixed voltage stress on HVDC converter wall-bushing simulated in PSCAD software for a 6-pulse rectifier.

3.2. The simulation was performed for the negative pole of the six-pulse rectifier end of the Manitoba Hydro HVDC Bipole 1. The voltage waveform has a direct voltage offset of nearly -400kV dc, and a fundamental alternating frequency component of 60Hz and approximately 120kV rms ac. It is apparent from the figure that there are considerable harmonics in this mixed voltage waveform.

An attempt was also made to measure the mixed voltage waveform. This measurement was performed by the use of a probe placed under the overhead conductor between the wall bushing and the valve-winding bushing of the transformer. In this measurement, only the time varying components of the voltage are induced in the measurement because it is not possible to induce the direct voltage component by this method. The mixed voltage waveform that was measured is shown in Fig 3.3. It is believed that the signal induced in the probe is coupling capacitive current from the overhead line. The signal shown in Fig. 3.3 appears to be the

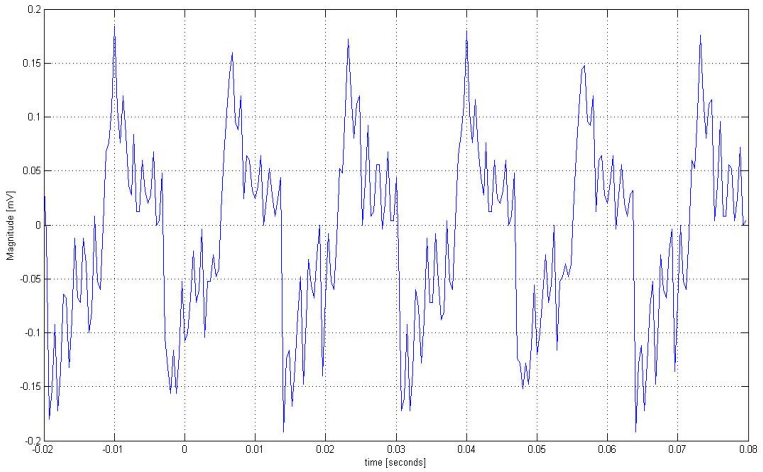

Fig. 3.3: Mixed voltage waveform measured by an antenna near the HVDC wall bushing overhead conductor

derivative of the simulated signal shown in Fig. 3.2.

To observe the harmonics present in the mixed voltage waveform the discrete time Fast Fourier transform was applied to the waveform as shown in Fig 3.4. From the discrete time Fast Fourier Transform we can see that the waveform has a large fundamental component at 60Hz. There are also large third, fifth, seventh, and ninth harmonic components, which are expected for the thyristor converter which is a six-pulse bridge converter. These harmonics act to stress the insulation and are considered in the analysis of the performed online PD measurements presented in Chapters 4 and 5.

Harmonics which are significant for the voltage stress on the wall bushing and valve-windings of the converter transformer are not as significant for the line-windings of the converter transformer. This is because most of the large harmonics

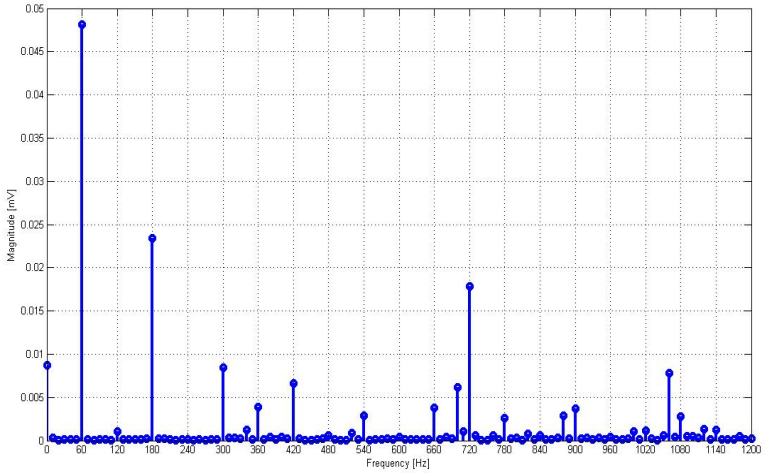

Fig. 3.4: Discrete Time Fast Fourier Transform of mixed Voltage waveform measured by probe near the HVDC wall bushing overhead conductor

are absorbed by odd harmonic filters and synchronous machines terminated on the same ac bus as the line winding. The direct voltage offset is also removed in the transformed voltage. Therefore, the voltage waveform stressing line-winding insulation is considered mostly sinusoidal because most of the large harmonics are filtered by the transformer inductance. As a result, the data obtained from online PD measurement may be analyzed with the use of phase-resolved PD patterns. There is however, the possibility of discharges occurring inter-winding, meaning between the valve-winding and line-windings of the transformer. In this case, the transient and harmonic voltage stresses may have to be considered when analyzing the measured PD data.

3.3 Characterization of the Noise Environment

The largest source of electromagnetic interference in the HVDC station environment is due to the regular switching of the twelve-pulse thyristor controlled HVDC converter. In Fig. 3.5, a phase-resolved plot of the repetitive switching noise caused by twelve-pulse converter that was measured from an HVDC wall-bushing is shown. The twelve pulse converter will produce switching pulses twelve times per 60-Hz cycle [20]. As a result, the measurement of the interference in Fig. 3.5 shows twelve distinct pulses that are equally spaced, occurring repetitiously over the 60-Hz interval. Because these pulses occur at the exact same phase locations repetitiously they are identified as noise. This measurement was acquired from an online PD measurement performed on the valve-windings of a converter power transformer. The method of coupling for the measurement was on the valve-winding bushing capacitance tap.

The produced switching noise creates a dilemma for the online measurement of PD. The measurement instruments will have poor signal to noise ratio, and furthermore because the interference is so repetitious it can blind the measurement of actual PD which is occurring close in time to the switching pulses. Fig. 3.6 shows the spectrum of pulse activity that was measured in the frequency range between 0-30MHz. Measurements were performed at three different locations, the wall-bushing, the transformer valve-winding, and the transformer line-winding (refer to Fig. 3.1). For each measurement the method of coupling into the insulation system

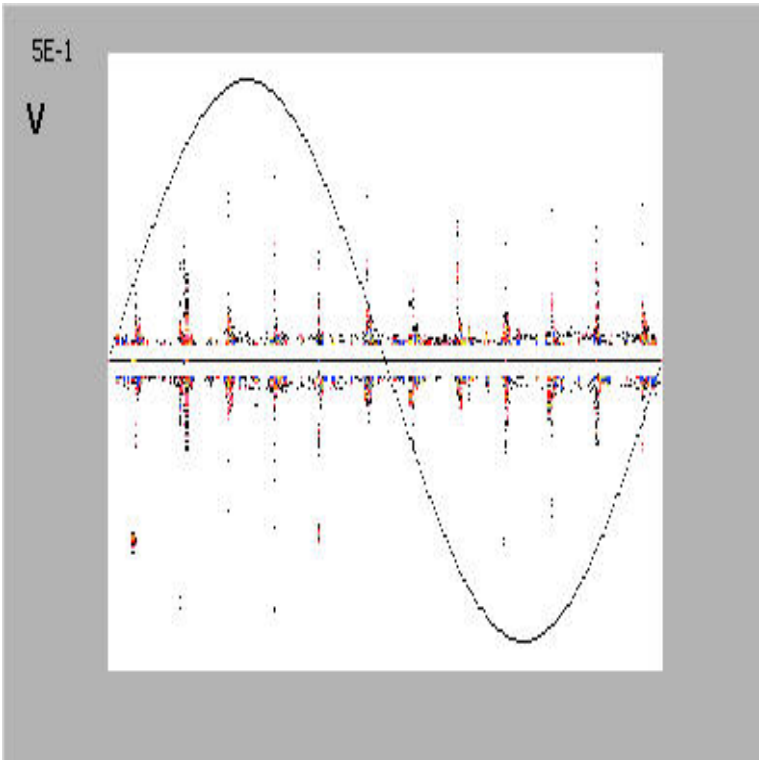

Fig. 3.5: Phase-resolved PD measurement of repetitive switching noise of the 12-pulse HVDC converter

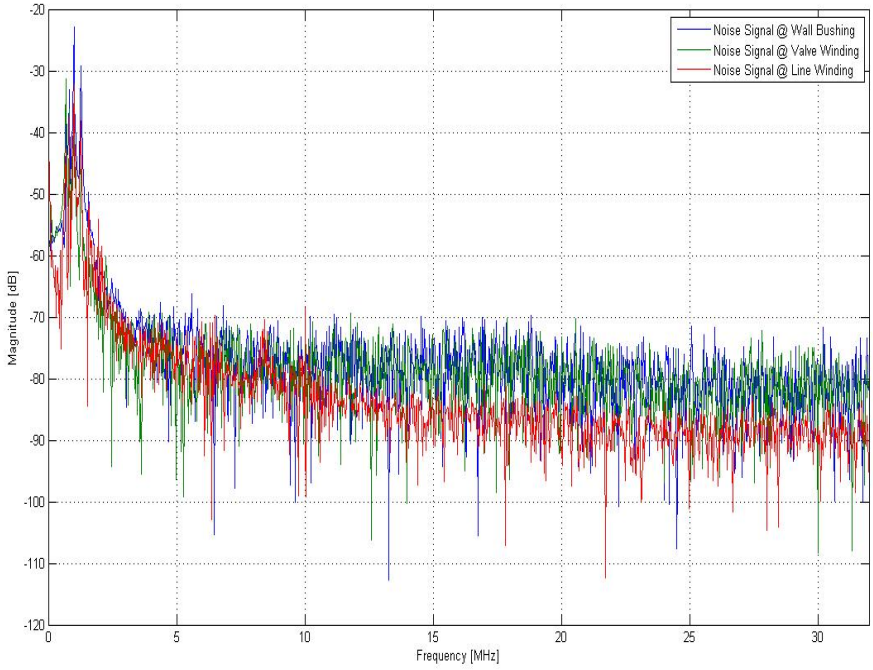

Fig. 3.6: Noise spectrum measured from wall bushing and transformer bushing capacitance taps

was the bushing capacitance taps, where each capacitance tap has a high-frequency current transformer terminated on its ground connection. The bandwidth of the high-frequency current transformer is approximately 400kHz-40MHz.

The noise spectrum in Fig. 3.6 shows that the maximum level of noise interference for all three measurement locations is around the frequency of 1.5MHz. The valve-winding and wall bushing are directly connected by the overhead line (Fig. 3.1) and therefore have similar magnitudes of interference over the entire noise spectrum.

In order to show the noise spectrum more clearly, in Fig. 3.7 the spectrum

signals have been smoothed with a best-fit polynomial (with order twenty). On the smoothed noise spectrum characteristic it is more clearly shown that the region around 1.5MHz is maximum interference. At this frequency the noise spectrum measured at the wall-bushing, and both transformer windings are all at maximums. Because this activity appears common in all three measurement locations, and the magnitude of the interference is so large, it is likely for this activity to be the switching noise. It is also noteworthy that signal is larger for the wall bushing than it is for the transformer winding measurements. This is due to the location of the wall-bushing being closer to the source of the interference, the valve converter. If we assume that the PD will have frequency content higher than 1.5MHz then the amount of interference in the online measurements may be reduced by the use of external filters. For the online measurements performed in this thesis, a 2.5-MHz second order high-pass filter was used to reduce the strong interference that is present in the bandwidth region near 1.5-MHz. The ideal filter characteristic is shown in Fig. 3.7. One can see that at frequencies above 2.5-MHz the level of interference from the switching noise will be improved.

In the frequency range between 10-MHz and 30-MHz the magnitude of the interference on the line-winding reduces. This suggests that the line-winding will have better measurement sensitivity for PD activity than the valve-winding. The valve winding and wall bushing are subjected to similar levels of noise by the converter.

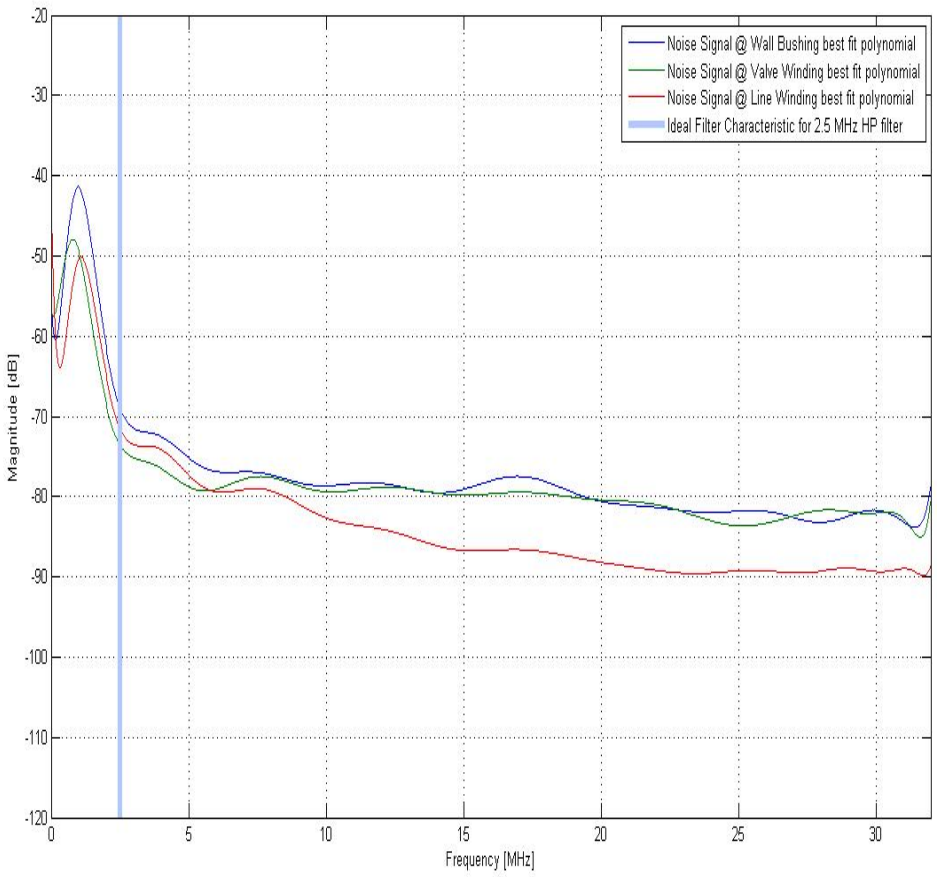

Fig. 3.7: Smoothed noise spectrum, shown with an ideal 2.5MHz High Pass filter characteristic

4. ONLINE MEASUREMENT OF PARTIAL DISCHARGES ON AN HVDC CONVERTER TRANSFORMER

Partial discharges occurring in a power transformer may be produced by a variety of possible defects. Due to the complexity of oil-paper insulation systems, discharges can occur within voids in the winding paper insulation, within gas bubbles in the transformer oil, or across surfaces of the pressboard barrier insulation, or in the associated bushings. It is important to be able to distinguish these discharge sources from one another because some discharge activity may indicate problems which are of greater risk for failure than others. For example, PDs occurring in bubbles in oil will degrade the insulating quality of the oil, but are not an immediate risk for failure. Whereas PD occurring in the winding paper insulation can promote conductive tracking paths along insulation surfaces that can cause an insulation failure much more quickly. PD in bushings is also hazardous. The inability to distinguish the source of PD greatly reduces the value of the measurement for the utility. Without identification, the information cannot contribute to decisions made for the maintenance of the transformer.

The transformer for which online PD measurements have been analyzed in this

Fig. 4.1: HVDC converter power transformer rated 262MVA, 60Hz, 230kV - 106kV, insulated for 500kVdc. This is a sister unit to the unit which had online PD measurements performed on it and is similar in appearance

work is similar to the unit shown in Fig. 4.1. The transformer is a 262 MVA, two-winding, three-phase unit. The transformer valve-winding is delta-connected and is connected to the HVDC thyristor controlled valve group (discussed in Chapter 3, arrangement shown in Fig. 3.1). The valve-winding is rated 106 kV (line-to-line) ac voltage, but is insulated for a direct voltage of 375 kVdc. The line-winding is star-connected and rated 230 kVac (line-to-line) and is connected to the 230 kVac bus of the inverter station. The line-winding has a grounded neutral star-point and is equipped with an on-load tap changer. A connection diagram of the transformer obtained from its nameplate is shown in Fig. 4.2. The valve-winding bushings are denoted X1, X2, X3 and the line-winding bushings are denoted H1, H2, H3.

In this chapter, the structure of the HVDC converter power transformer winding and insulation system are analyzed, for which an equivalent model is proposed.

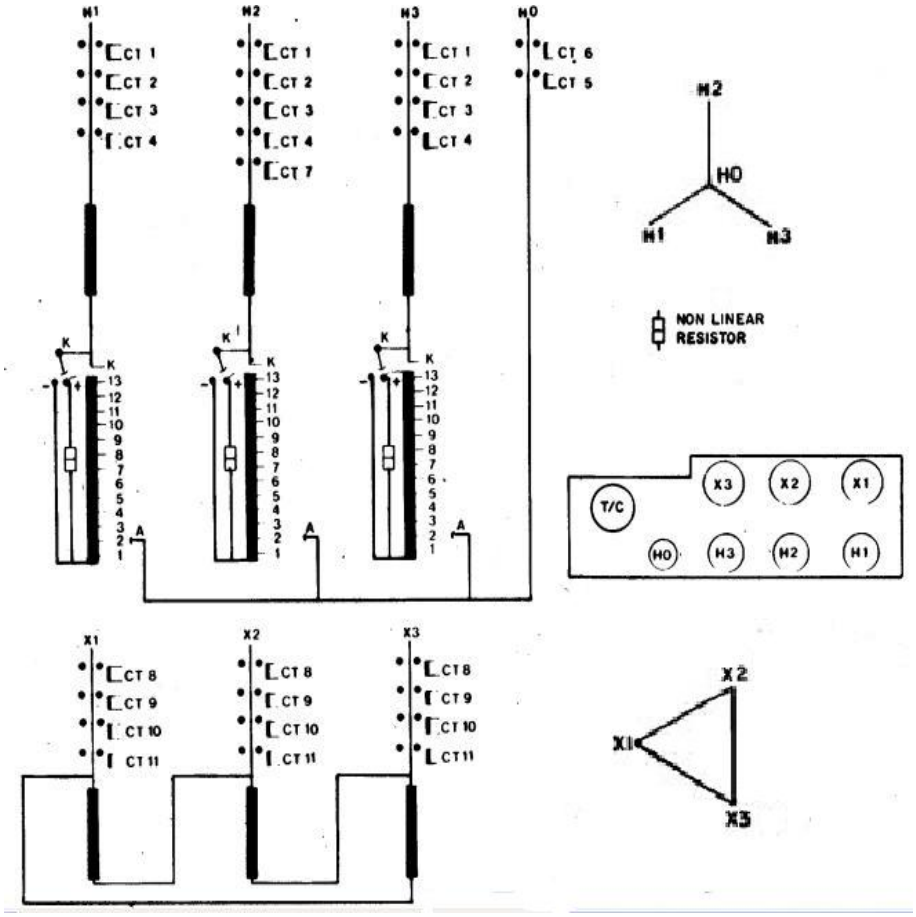

Fig. 4.2: HVDC Converter Transformer Nameplate Connection Diagram

The model is then used to aid in the description of a method of online PD measurement. The method is examined with regard for its measurement sensitivity to PDs occurring in the transformer winding. Additionally, the results from an experiment aimed at examining the influence of the PD pulse propagation distortions on the measurement of PD is presented and discussed. Lastly, data from actual online PD tests performed on the HVDC converter power transformer are presented and analyzed. The measurement data is post-processed with the aid of a feature extraction algorithm performed by the PDBase measurement instrument which is manufactured by the company Techimp Systems [21].

4.1 Structure of the Transformer Winding and Equivalent Model for Online PD Measurement

The construction of the transformer is such that the valve-winding is the outermost winding, closest to the steel tank walls of the transformer, and the line-winding is the innermost winding closest to the transformer core. Cylindrical pressboard barriers are located between the valve and line-windings, and between the valve-winding and the tank walls. The barriers are made of cellulose material and function to direct the circulation of the insulating oil in this directed oil-cooled design. The barriers also improve the electrical insulation level between the windings, and to the transformer tank walls.

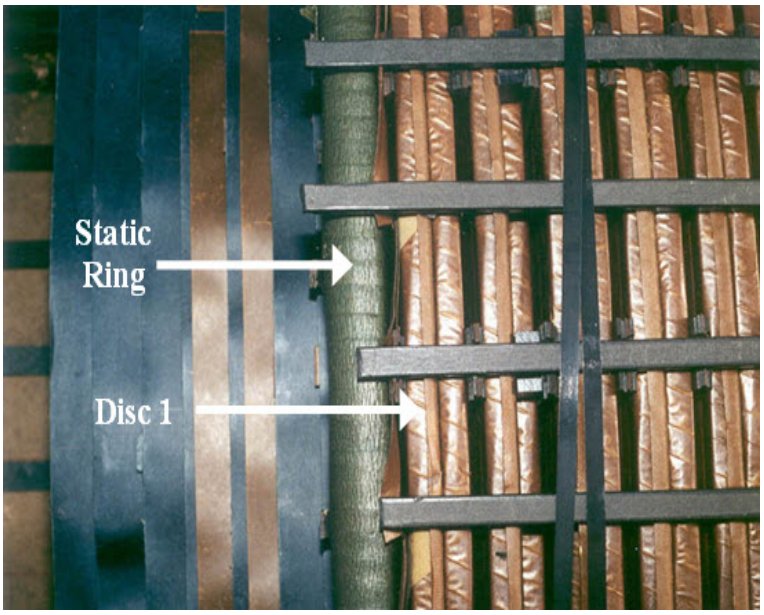

Fig. 4.3: Internal construction of valve-winding without oil.

Both transformer valve and line-windings are wound in discs which are constructed with turns of continuously transposed conductors (CTC). The individual conductors are copper strands insulated by an enamel coating. The winding CTC bundles are insulated with oil impregnated kraft paper. In Fig. 4.3, discs at the top of the valve-winding are shown with the unit drained of its insulating oil. Both line and valve-windings are similar in construction. In Fig. 4.3 the valve winding has a high-voltage static ring that is capacitively coupled to the turns of the top disc. The discs of the winding are configured such that there is no oil duct between disc 1 and disc 2, or between disc 3 and disc 4, etc. This is done to improve the series capacitance of the winding for voltage transient events that may occur in service.

The method of coupling for online PD measurements performed in this work is capacitive, achieved through capacitance taps on the transformer line and valve-winding bushings. The bushings are a condenser-type insulation which has oil impregnated aluminum foil paper layers concentrically wrapped around the central bushing conductor. The capacitance tap is located at the grounded flange of the transformer bushing. This tap is electrically connected to a condenser layer that is second from the outermost condenser layer at the bushing flange. The capacitance tap exists to allow for off-line maintenance diagnostic tests to be performed on the transformer bushing. In service, this tap must be grounded, however, it may serve as a capacitive coupler for PD measurement by grounding the tap through a high frequency current transformer. In Fig. 4.4, a high frequency current transformer (HFCT) is shown installed at the grounded bushing capacitance tap. The HFCT has negligible impact on the grounding and provides a channel for the high frequency content of PD pulses that propagate through the winding. To monitor for PD online on the HVDC converter transformer, HFCTs are installed on each phase of the valve and line-windings.

An equivalent transformer model for the performance of online PD measurement is proposed as shown in Fig. 4.5 [22]. The equivalent circuit shown is intended to represent the transformer valve-winding and has a static ring which capacitively couples with the top winding disc. The line-winding would be modeled similarly.

In the winding, each disc may be modeled as a series inductance and resistance.

Fig. 4.4: Method of PD coupling through High Frequency Current Transformer terminated on the capacitance-tap of the line-winding transformer bushing

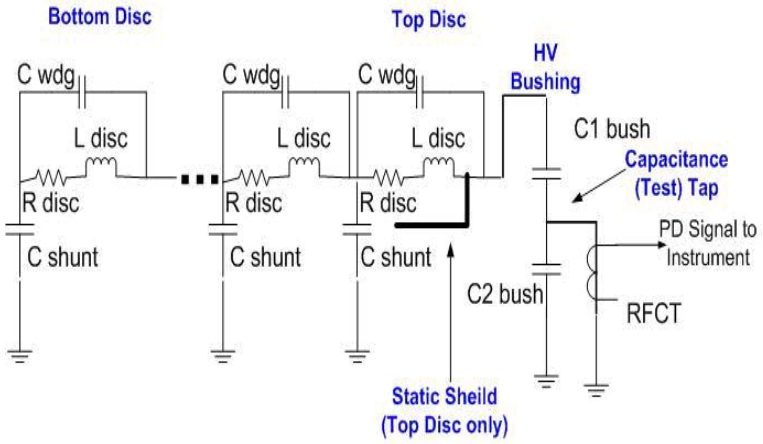

Fig. 4.5: Equivalent transformer model with method of PD coupling

The discs also have a shunt capacitance to the transformer tank, core and the opposite winding. Also, parallel to the series inductance and resistance, there exists an inter-turn and inter-disc series capacitance. This distributed model is a repeating structure from the top disc down for as many discs as are present in the winding. The bushing capacitance tap is modeled as two capacitors, where C1 is the capacitance between the high-voltage lead and the tap, and C2 is the capacitance between the tap and the ground flange of the bushing which is bolted to the transformer. The tap is grounded in service through the HFCT. The signal from the HFCT is routed to an online PD measurement instrument through a coaxial cable with 50 ohm surge impedance.

4.2 Measurement Sensitivity for PD Signals Occurring in the Transformer Winding

The capacitive method of coupling on the transformer bushing has an impact on the measurement sensitivity for PDs occurring in the transformer winding. For an online PD measurement with the method of coupling shown in Fig. 4.5, the transfer-function for discharges occurring in the winding and measured by a test instrument with an impedance R is:

$$T(j\omega) = \frac{PD_{meas}(j\omega)}{PD_{winding}(j\omega)} = \frac{j\omega RC_1}{(1 + j\omega RC_2) + j\omega RC_1} \tag{4.1}$$

The bushing capacitances for the transformer studied in this work are approximately C1=475pF, C2=13000pF on the valve-winding bushing and C1=510pF, C2=7100pF for the line-winding bushings. The input impedance of the test instrument is approximately 50 ohms. Given these parameters, calculated magnitude responses for the bushing capacitance tap method of coupling on the valve and line-windings are shown in Fig. 4.6.

The bushing capacitance tap essentially functions as a high-pass filter for the high-frequency content of the PD pulses. The magnitude response demonstrates that this method of coupling has good sensitivity for signals above 420 kHz. At frequencies below 420 kHz the signals become highly attenuated by the bushing capacitance. The magnitude of frequency response shows that the line-winding bushing has better sensitivity for PDs, with an attenuation level of -23.5dB for signals above 420 kHz. The valve-winding attenuation is approximately -29dB for signals above 420 kHz.

In addition to the capacitive coupling, the HFCT also has an influence on the transmission of the induced PD current signal. The HFCTs used for coupling the measurements are manufactured in-house by Manitoba Hydro technicians. The HFCTs consist of a split-core ferrite and a four-turn secondary winding. The magnitude response for the HFCT was measured experimentally in a bench-test. A signal generator was used to inject current signals into the primary of the HFCT over a range of frequencies. The output was measured on the HFCT secondary

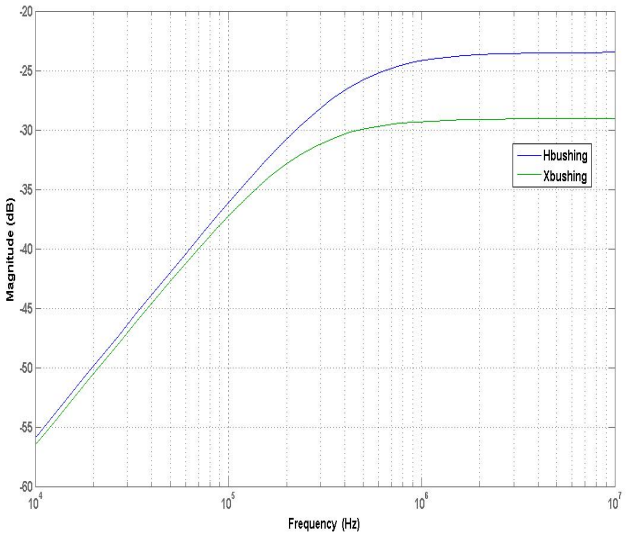

Fig. 4.6: Calculated Magnitude Frequency Response for Valve (Xbushing) and Line (Hbushing) Winding Bushings and associated 50 ohm surge impedance termination

with an oscilloscope. The magnitude response of the HFCT is shown in Fig. 4.7.

The HFCT has a flat frequency response in the range between 400kHz - 40MHz. Therefore, the entire method of coupling (bushing capacitance tap and HFCT combined) for online PD measurements, has good measurement sensitivity for PD signals in the frequency range between 420kHz - 40MHz. The HFCT response becomes erratic at frequencies above 40MHz. This is believed to be caused by influence from the signal cables and stray capacitances in the circuit.

The measurement instrumentation that has been used for the online acquisition of PDs occurring in the power transformer, is designed for wideband acquisition, and is capable of measuring PD data in the frequency band up to 30MHz.

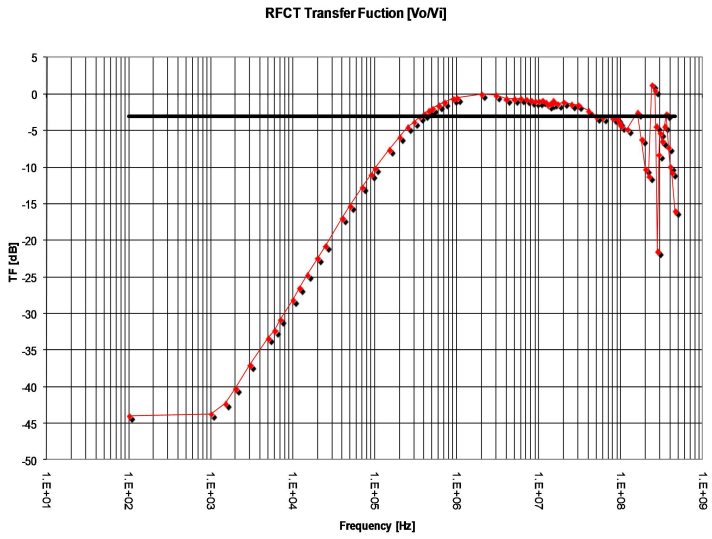

Fig. 4.7: Magnitude response measured experimentally for a High Frequency Current Transformer

Therefore the method of coupling which we have determined as falling within the frequency range of 420kHz - 40MHz, is suitable for supporting the measurement instrument that will be used for the online PD measurement.

In Chapter 3, it was determined through the characterization of the noise environment that a 2.5 MHz high-pass filter should be installed at the input channel of the measurement instrument. This filter was installed to reduce the interference from the thyristor switching events. Therefore, the frequency range in which online PD measurements were acquired in this work is constrained to the range between 2.5MHz-30MHz.

This limitation at the lower frequency band affects the depth at which the transformer winding may be monitored. Because the transformer impedance is

largely inductive it will attenuate higher order frequency content. If PDs occur deep within the winding, their frequency components which are 2.5MHz or higher may be attenuated by the inductive elements of the winding to the extent that they do not appear in the PD measurement.

4.3 Influence of the Winding and Partial Discharge Propagation Distortions

Partial discharge pulses occurring in the transformer are influenced by distortion when the pulses propagate through the transformer, away from the site of the discharge activity. To examine the effects of propagation distortion in this thesis an experiment was performed on a power transformer specimen without oil. This transformer specimen has a 250kV star connected valve winding is a different converter transformer from the one which is described at the beginning of this chapter, and is of an earlier design than the delta unit on which the online PD measurements were made. This transformer had previously failed due to a turn-to-turn fault in its B phase valve-winding.

An experiment was performed on the intact C-phase valve-winding. To perform these tests, the transformer oil was drained, and layers of the pressboard material were removed to uncover the discs of C-phase valve-winding, shown in Fig. 4.8 . A pulse generator, normally used as a PD calibration device was ground referenced

Fig. 4.8: C-phase valve-winding discs exposed to perform pulse injection response tests.

to the inner tank wall of the transformer. Pulses were injected into the winding discs through a differentiating capacitor of 100 pF to simulate PD. The risetime of the pulses was approximately 4 nanoseconds. Pulses were injected beginning at the top disc (disc1) closest to the bushing and sensor, and then progressively at discs deeper in the winding.

The PD pulse injection responses, measured from the HFCT sensor are shown in Fig. 4.9. The attenuation for injections at discs further into the winding is noticeable. It is also noticeable that there is a distortion of the pulse shape.

Distortion may also be observed in the frequency domain. A Fast Fourier Transform (FFT) was performed and plotted in the frequency range between 0 and 30-MHz. The magnitude response in Fig. 4.10 shows that at higher frequencies

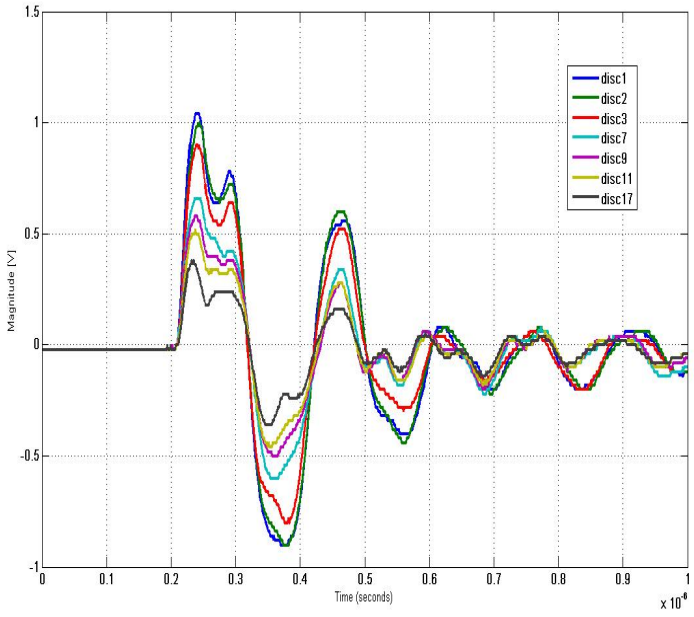

Fig. 4.9: Pulse injection responses for injections at various winding discs.

the amount of attenuation is not directly proportional to the propagation distance of the traveling pulse. Around the 5-MHz frequency the relationship between attenuation and propagation distance appears to be proportional, however, above 12-MHz there is very little difference in the attenuation for propagation distances between discs 1-9. These findings are similar to those previously documented in [23]. The attenuation of a PD pulse propagating through a transformer is a function of the frequency content in the initial pulse waveform, and the propagation distance.

The distortion of the pulse waveforms is also caused from dispersion effects. Dispersion happens when the phase velocity of some spectral components are faster

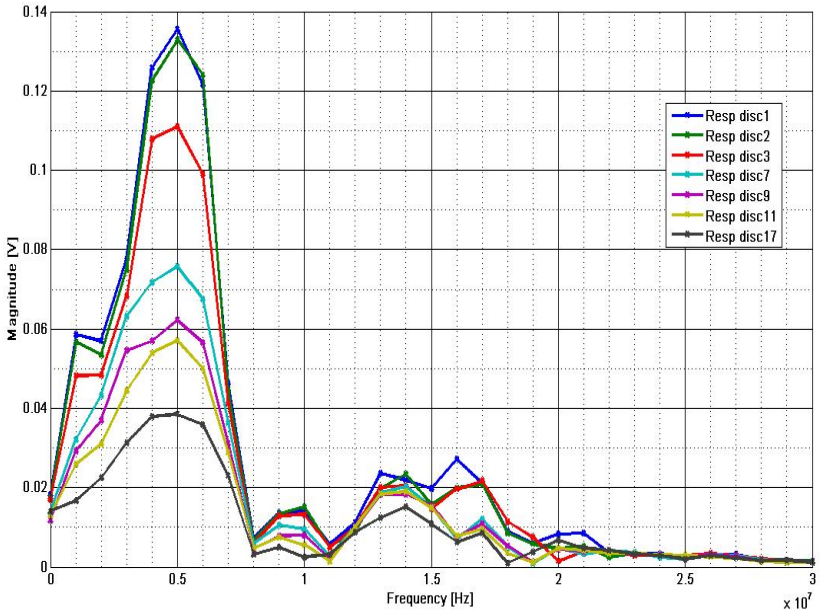

Fig. 4.10: Magnitude response (Range 0-30MHz) for pulse injections at various winding discs.

than the overall group velocity. The result is a distortion by spreading of the pulse waveform as it propagates through a medium. The effects of dispersion are evident in Fig. 4.11, which shows the phase response in the frequency range between 4 and 9-MHz. At frequencies above 7-MHz, dispersion becomes evident. The pulses with longer propagation distances, begin to phase-lead pulses that were injected closer to the HFCT sensor. This is because for injections further into the winding, the higher frequency components of the PD pulse arrive at the HFCT sensor sooner than the lower frequency components. The data suggests that the frequency content of the original PD pulse that are above 7 MHz are more likely to propagate across the inter-disc capacitive regions, which is a shorter path to the HFCT sensor, and frequency components below 7 MHz propagate through the longer path of the winding conductor. This causes a spreading of the spectral components, which is dispersion.

The attenuation and dispersion of PD pulse waveforms are potentially significant for some modern on-line partial discharge measurement instruments. These modern instruments use fast sampling digital oscilloscopes to capture PD waveforms and analyze the data using feature extraction algorithms that identify characteristics of the PD pulse shape [17, 18].

Here, a method of moments feature extraction algorithm is applied to the pulse response data gathered from injections at various disc locations of the salvaged power transformer. Equations for the feature extracted parameters, equivalent

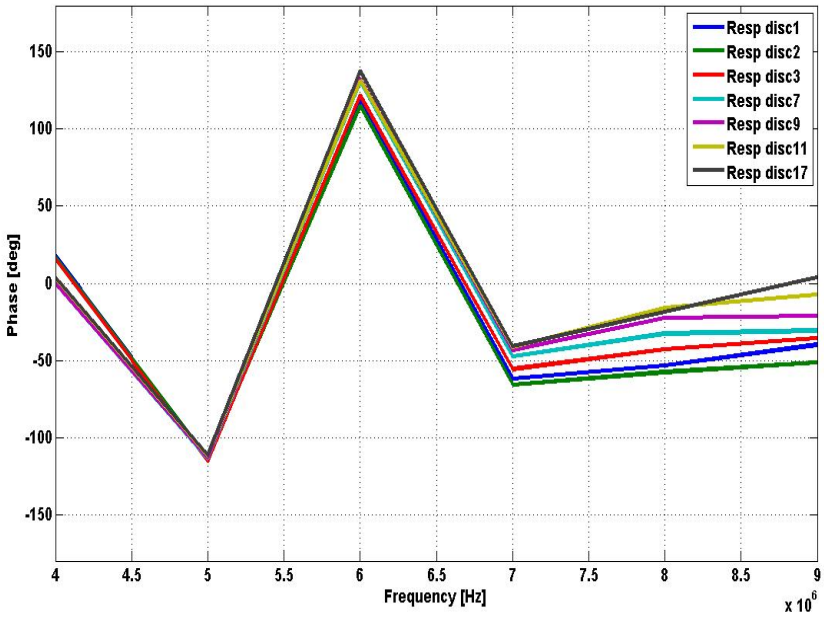

Fig. 4.11: Phase response for pulse injections at various winding discs. Dispersion after 7 MHz

time-length and equivalent bandwidth, were defined in chapter 2, section 2.5.5. The algorithm was applied to the pulse waveform data through post-processing that was performed in MATLAB software.

The TW-plane shown in Fig. 4.12 is produced by processing the pulse data using the feature extraction algorithm. The parameter for equivalent time-length (defined in Eq. 2.8) appears to increase as propagation distance increases because of the influences of dispersion on the pulse waveform. The normalized quantity for equivalent time-length T, increases as a function of the duration of the time-domain signal for the PD pulse. Therefore as dispersion contributes to the spreading of the pulse waveform, equivalent time-length is increased. The equivalent bandwidth, W (defined in Eq. 2.9), also appears to increase as a function of propagation distance. The normalized quantity for equivalent bandwidth W, increases as a function of the magnitudes of the frequency components. For injections deeper in the winding, there is relatively less attenuation of the high frequency components, versus the lower frequency components. This will contribute to increasing the equivalent bandwidth.

These results are significant because they suggest a relationship between propagation distance and the parameters for equivalent time-length and equivalent bandwidth. This relationship can aid in the interpretation of online PD measurements performed on power transformers. Based on the shape of the cluster produced, it can be determined whether a defect producing discharges in the wind-

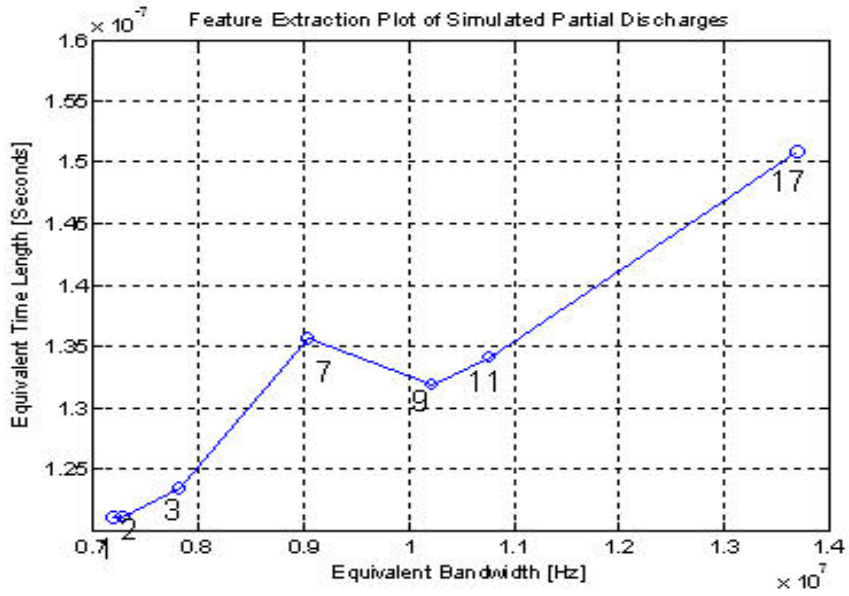

Fig. 4.12: Phase response (Range 0-30MHz) for pulse injections at various winding discs.

ing insulation is acute, meaning that PD activity is located at one specific region of the winding, or distributed, meaning the PD activity is occurring along a region of the winding. If the cluster produced from an online PD measurement is largely dispersed, having a large variation in equivalent time-length and equivalent bandwidth, then it is likely a distributed defect along a portion of the winding. However, if a cluster is local to one region of the feature extraction map, and has little variation in equivalent time-length and equivalent bandwidth then the defect is likely acute.

On the feature extraction map, the location of a cluster from a PD measurement may provide information about the location of a defect along the winding. Because the feature extraction parameters appear to vary proportionately to the

propagation distance in Fig. 4.12, this can provide information about the relative location of the defect. This is potentially valuable for corrective maintenance. Assume for example that a PD acquisition and feature extraction method produce a cluster of PD pulse data that has relatively low equivalent time-length, low equivalent bandwidth, and that the cluster is very densely dispersed. Because the equivalent time-length and bandwidth are relatively low it may be assumed that the propagation distance in the winding is somewhat short. Also because the cluster of pulses is very densely distributed the defect is likely acute. The location of the defect may be interpreted from the data as occurring near the top of the winding and close to the high voltage bushing. Depending on the type of transformer, this type of defect may be accessible during a maintenance outage and repaired.

4.4 Results from Online Partial Discharge Monitoring

Online PD measurements were performed on an HVDC converter transformer (described at the beginning of this chapter) on seven different occasions over a period between July 20, 2007 to October 1, 2010. Each measurement session was performed with discrete acquisitions taken from a single winding at a time. The data was acquired in the form of a phase-resolved measurement, where the reference signal was provided from a station voltage transformer that was in phase with the A-phase line-winding. Each session involved performing discrete PD measurements

on each of the six transformer windings, via the method of coupling with HFCTs installed on the winding bushing capacitance taps. The data was later processed and analyzed with the aim of identifying the nature of the PD phenomena occurring in the transformer. The test instrument used was the PDBase, manufactured by Techimp Systems. This instrument implemented a feature extraction method (described in Chapter 2, Section 2.5.5) that was capable of isolating individual PD phenomena occurring within the transformer.

4.4.1 Analysis of the Line-Winding PD Measurements

The line-winding measurements are analyzed by using the feature extraction method to isolate individual PD phenomena. The isolation produces phase-resolved PD plots for each individual phenomena. Identification of the individual defects are done so by comparing the phase-resolved PD plots, with patterns produced in documented laboratory experiments performed in [14, 24, 25].

These laboratory experiments produced phase-resolved PD patterns for test specimens that were constructed to simulate certain transformer insulation defects. The simulated defects were designed to produce phase-resolved PD patterns that would be similar to those caused from actual PD occurring inside of a transformer. For example in [24], to simulate discharges in oil from a high field stress region on the transformer winding, a point-plane gap was placed in a glass cylinder and filled with insulating oil. The point-plane gap was put under alternating voltage stress

and a phase-resolved PD pattern was recorded. Similarly, patterns were generated in [24] by simulating defects for PD occurring at the surface of pressboard material, PD occurring in the winding paper insulation, and PD occurring in response to contaminants in the oil. These simulated patterns from laboratory experiments are produced with the purpose of comparison with real in-field measurements of PD, for the identification of the defects which cause PD.

In addition to simulated PD patterns from laboratory experiments, an understanding about the physics of insulation defects under alternating voltage stress can aid in identification of PD activity in the line-winding. For example, if discharges are produced by a void in the winding paper insulation. The walls of the void are composed of the same dielectric materials (oil-impregnated paper) which will produce a symmetrical discharge pattern. By symmetrical it is meant that the magnitudes of the PD pulses, and their repetition rate will be similar for the positive and negative half cycles of the alternating voltage waveform. Alternatively, when the site of the defect is at a boundary or interface between two dielectric materials, the phase-resolved PD pattern will be asymmetrical. An example of such a defect might be discharges off the surface of the transformer pressboard barrier, into the insulating oil.

Another quality of phase-resolved PD patterns under alternating voltage stress, are that the distributions of PD pulse magnitudes are expected to be roughly centred at the 45-degree and 225-degree phase-angle locations. Also, the phase

distribution of the PD pulse magnitudes will normally fit a Weibull or Gaussian type distribution (Fig. 2.5) as was explained in Chapter 2 [11,12]. This information can be used to determine whether the discharge activity is occurring on the phase for which it was measured on, or if it is from an external source. For example if the phase angle locations of a Gaussian distributed phenomena are not located at the 45 and 225-degree locations of the phase-resolved plot, they are likely caused by PD on another transformer winding that is cross-coupled into the measurement.

An example of one online PD acquisition performed on the A-phase, line winding is shown in Fig. 4.13. The full phase-resolved PD measurement is shown in the upper left column of the figure along with its corresponding feature extraction classification map shown on the lower left. Clusters of PD pulses produced from the feature extraction are shown on the classification map and the separation of the clusters was performed in the post-processing and analysis of the data. Each separate cluster, as shown, correlates to a single defect, or PD phenomena for which a phase-resolved PD pattern is produced. In this acquisition there appear to be five distinct defects producing discharge.

The PD phenomena in Fig. 4.13, denoted **(a1)**, corresponds to a cluster located at approximately 5.5-MHz equivalent bandwidth and 1050 nanoseconds equivalent time-length on the feature extraction map. The phase-resolved PD pattern, for discharges associated with cluster **(a1)** is shown in the top right column of Fig 4.13.

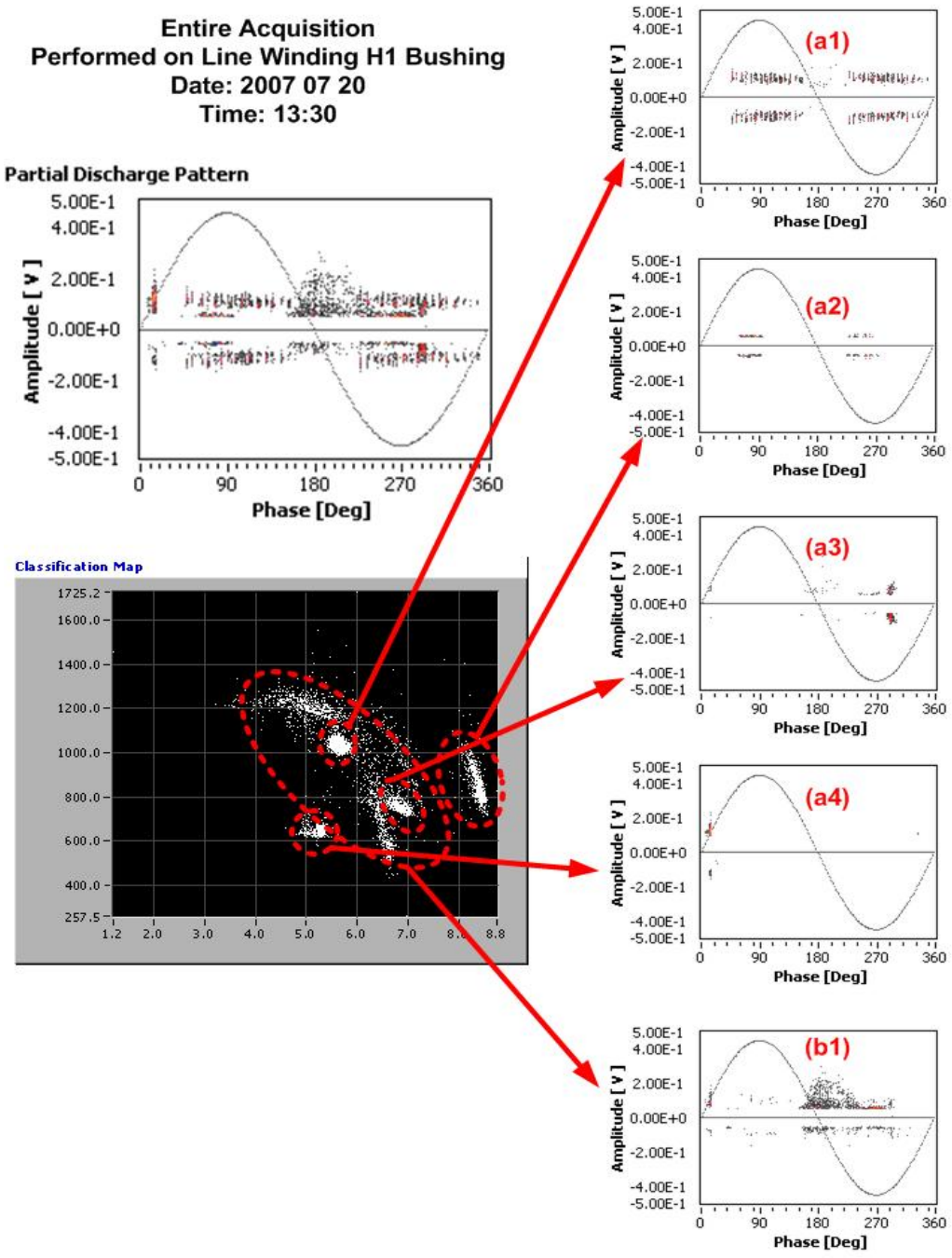

Fig. 4.13: Feature Extracted PD data from online acquisition performed on 2007 07 20. There are a total of 5 distinct phenomena observed in the acquisition.

The phenomena **(a1)** is not a typical discharge pattern for defects in oil-paper insulation systems under alternating voltage stress. The PDs appear to come in short intermittent bursts of equivalent pulse magnitudes. The distribution of pulses with respect to phase-angle are similar for both positive and negative half cycles of the sinusoid, but do not resemble a Weibull type distribution. Because of this, the source of the discharges is not attributed to the line-winding. These discharges could be associated with cross-coupling from discharges occurring on the valve-winding. Or alternatively, the discharges could be associated with inter-winding stresses between the valve-winding and the line-winding. Influence of the valve-winding in producing these discharges is suspected because the pattern of pulses appear in short bursts of activity. The repetitious short bursts of discharge appear to suggest that the phenomena could be in response to a harmonic component of the valve-winding voltage stress produced from the thyristor controlled converter(Fig. 3.4). It is also noteworthy that the cluster of pulse data appearing in the feature extraction map is very densely distributed. External noise interference can produce a dense cluster on the feature extraction map because the source of the electromagnetic interference is unchanging, unlike PD which is somewhat more stochastic in nature. However, this same pattern may have been produced by an acute defect on the valve-winding and cross-coupled into the line-winding measurement.

The next phenomena denoted **(a2)**, has relatively low magnitude and repetition-

rate making it somewhat difficult to identify based on pattern. The phase-resolved PD pattern information shows a roughly Gaussian distribution of pulse magnitudes which are centered at the 45-degree and 225-degree phase locations. The distributions are also roughly symmetrical between the positive and negative half cycles. This information suggests that this phenomena is due to internal PDs attributed to the A-phase line-winding. The fact that the PD pulses appear similar in magnitude for the positive and negative half cycles suggest that the PD may be occurring in voids in the winding paper, or pressboard layered insulation.

Defects **(a3)** and **(a4)** appear not attributed to PD activity, but instead from switching noise cross-coupled from the valve-winding. Because the phase-resolved PD patterns are not Weibull distributed, and not centered near the 45 and 225 degree phase-angle locations, these discharges are not occurring in response to the line-winding voltage stress. Furthermore, the clusters of pulse data for **(a3)** and **(a4)** are very densely distributed on the feature extraction map, suggesting they could be produced by external noise. Also, the phase-resolved pattern for these discharges resemble those shown in the HVDC noise pattern in Chapter 3, Fig. 3.5.

Defect **(b1)** shows a Gaussian type distribution of phase-resolved data, however the phase angle location of these discharges are not centered at the 45 or 225-degree phase-angle locations. Therefore it can be concluded that the activity in **(b1)** is not native to the A-phase winding because the activity is not responding to increasing

portions of the line-winding voltage stress. This phenomena is 120-degrees lagging the 45-degree phase location, and can therefore be attributed to B-phase winding.

The analysis of this acquisition demonstrates that isolation of the PD phenomena by the method of moments feature extraction, enables the interpretation of individual PD data. It becomes easier to identify the nature of the defect causing discharge.

Data from the online PD measurements performed on the line-windings B and C phases on July 20, 2007, are shown in Fig. 4.14. The B-phase acquisition shows a single defect **(b1)** that can be attributed to PD on the B-phase winding. This activity has a Gaussian type distribution and is centered at the 45-degree phase angle location of the B-phase line-winding voltage. Because the pattern is asymmetrical for the positive and negative half-cycles of the sinusoid, it suggests that the defect is at a boundary or interface between two materials in the insulation system. Defects such as voids have symmetrical phase-resolved PD patterns because the transfer of charge under one polarity of voltage stress is identical to the transfer in the opposite polarity. This is because the materials are the same for the direction of discharge under both positive or negative electric stress. At a defect located at a boundary in the insulation (such as discharges from the winding into the oil, or discharges along a pressboard barrier surface), the transfer of charge differs depending on the polarity of the electric stress. This is because different materials on either end of the defect will cause different discharge current

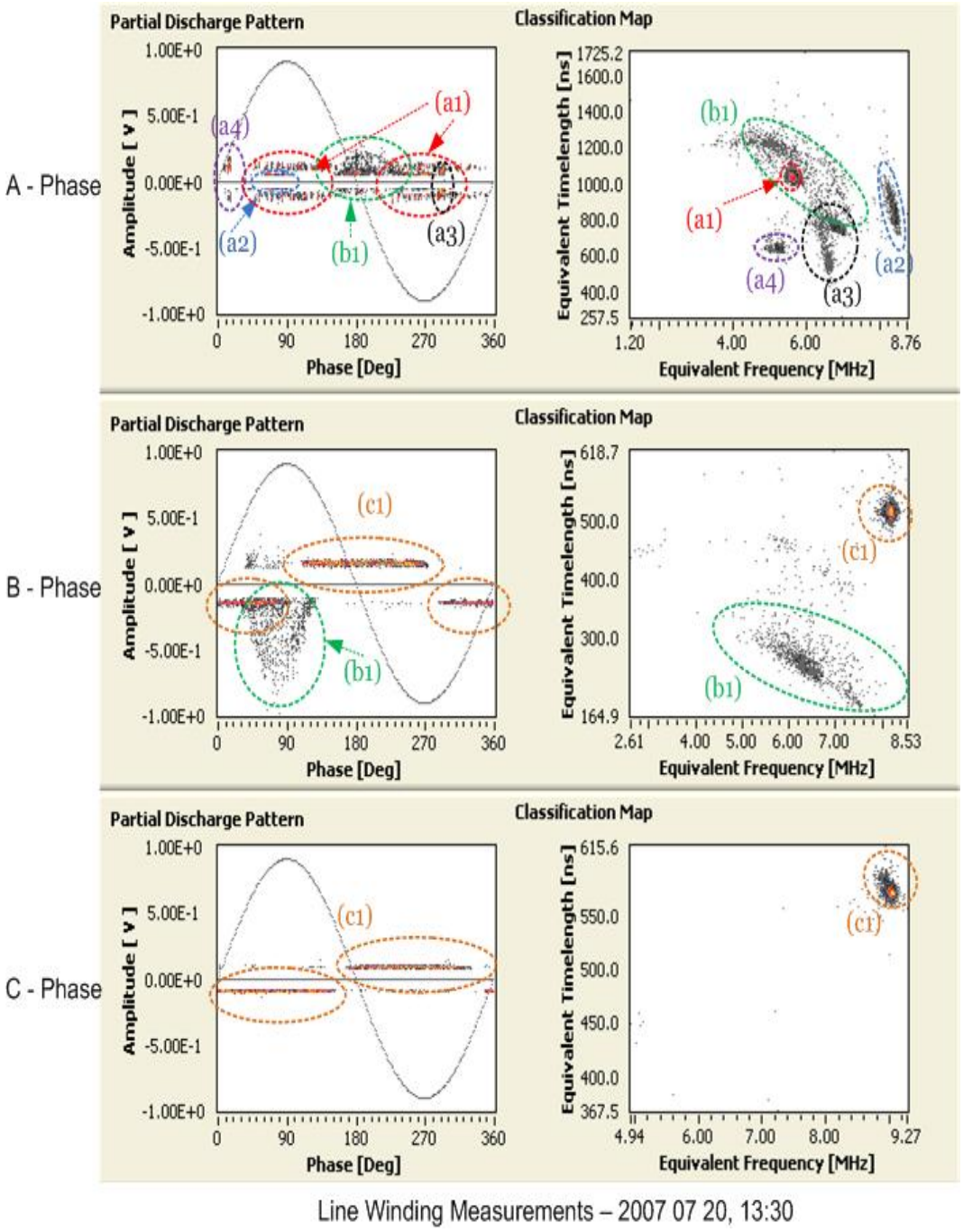

Fig. 4.14: Online line-winding measurements performed on 2007 07 20

pulses under positive or negative electric stress. In this case, the discharge pattern for **(b1)** appears to be either discharges along a pressboard barrier surface, or a corona type discharge occurring in the oil from a high field-stress region on the winding. This identification is based on the resemblance of **(b1)** to patterns that were obtained from laboratory tests in [24].

The defect denoted **(c1)** in Fig. 4.14 appears to be attributed to discharges occurring on the C-phase line-winding. Although the magnitude distribution of pulses are flat, and not a clear Gaussian or Weibull type distribution, they are roughly centered at the 45 and 225 degree phase angle locations. Because the pattern **(c1)** is symmetrical on the positive and negative half cycles, it suggests that the phenomena may be caused by PD at voids in the winding insulation or pressboard material. The feature extraction map shows a very densely distributed cluster of pulse data, which could suggest the phenomena is noise, but because no similar pattern is observed on the A or B-phases this is considered unlikely. As a result, the source of the phenomena **(c1)** appears to be from an acute void defect in either the winding paper insulation, or pressboard material.

4.4.2 Analysis of Valve-Winding Measurements

Online PD measurement discharge patterns for the valve-windings as performed on July 20, 2007 are shown in Fig. 4.15. The interpretation of these patterns are challenging for a number of reasons. The first reason was mentioned in Chapters

2 and 3, that the valve-winding is stressed by a mixed voltage waveform, having direct, alternating and switching transient components. Discharge may occur in response to any one of these stresses. Although the data in Fig. 4.15 displays a clean sinusoidal voltage waveform, the real waveform is more similar to that which has been shown in Fig. 3.2. The voltage reference which was obtained from an auxiliary voltage transformer, in phase with the A-phase line-winding, has been corrected for a 30-degree phase-shift associated with the delta-connected valve-winding. Another challenge for online PD measurement of the valve-winding is the significant electromagnetic interference on this winding from the thyristor switching operations of the HVDC converter. Finally the last reason the online PD measurements on the valve-winding are challenging, is that the measurements, in general have very low magnitude pulses and low repetition-rates. This makes the identification more difficult.

In Fig. 4.15, the A-phase valve winding is characterized by two different discharge phenomena. The phenomena **(a1)** may be caused by discharges in voids in response to a harmonic component of the voltage waveform. On the phase resolved pattern for the A-phase valve-winding the pattern shows a phenomena that clearly extinguishes during polarity transitions (zero crossings) of the 60-Hz alternating voltage component. This supports that the phenomena is native to the A-phase valve-winding. The phase-resolved PD pattern also shows both positive and negative polarity pulses which suggests that the phenomena may not be attributed to

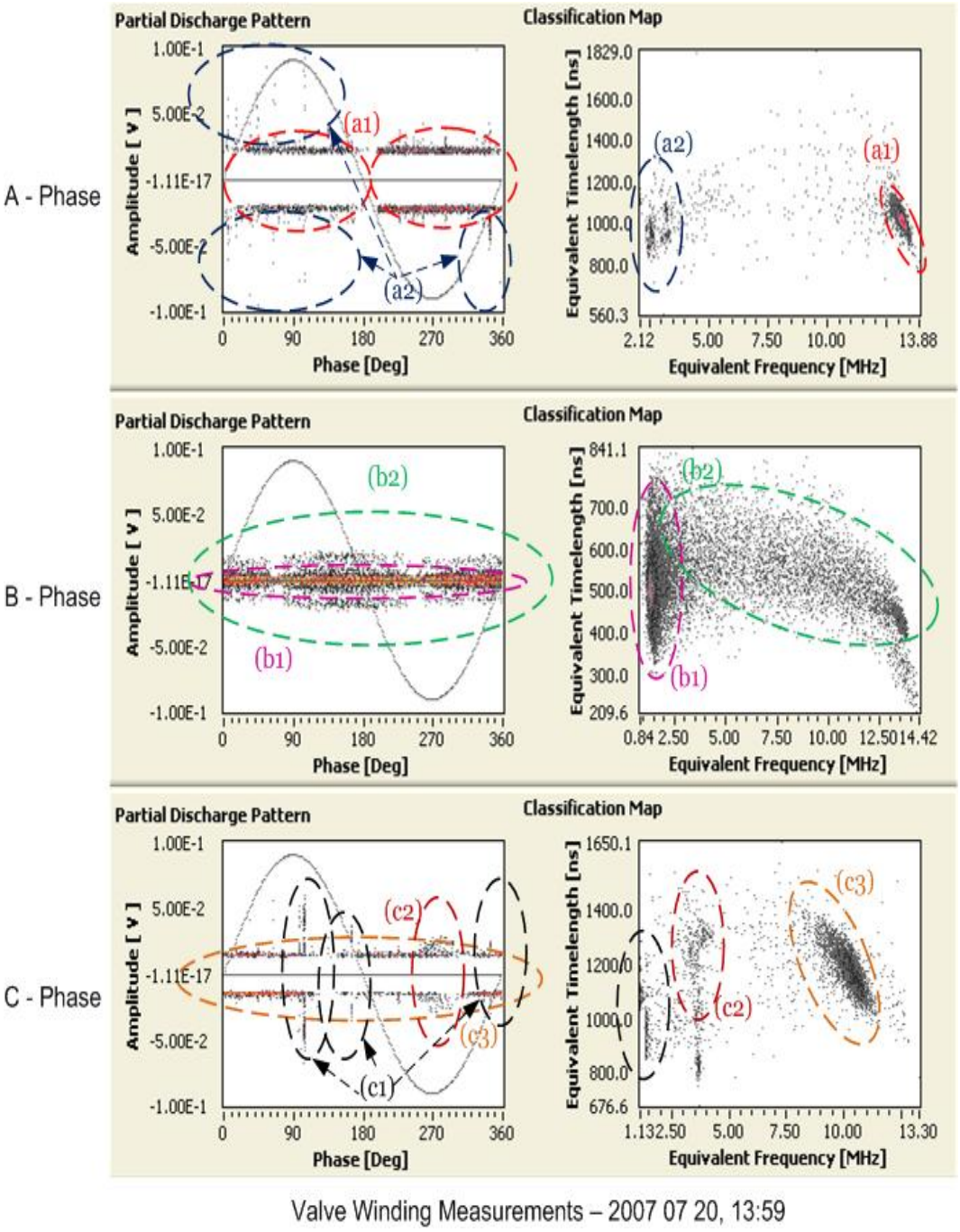

Fig. 4.15: Online valve-winding measurements performed on 2007 07 20

the direct voltage stress portion of the voltage waveform. Discharges in response to direct voltage stress would be unipolar. Because the positive and negative polarity pulses appear to be mirror images of each other over a 60-Hz interval, suggests that the recurrence of the discharges are caused by a frequency component that is faster than 60-Hz component of the voltage waveform. A harmonic component excited by the converter switching could have caused this more rapidly recurrent PD pattern for **(a1)**.

The other phenomena captured on the A-phase valve winding, denoted **(a2)** appears to be switching noise from the thyristor converter. This is because the magnitude distribution of it phase-resolved plot is very narrow, and the pattern resembles the switching interference shown in Chapter 3, Fig. 3.5. It is also noteworthy that the equivalent bandwidth of this phenomena is relatively low which also supports that the phenomena **(a2)** in Fig. 4.15 is noise.

The B-phase valve-winding feature extraction produced two phenomena which appear related, however, these phenomena are not attributed to the B-phase valve-winding. The phase-angle locations for **(b1)** and **(b2)** do not correlate to the B-phase valve-winding voltage stress because the gaps in the discharge activity do not correlate to the zero crossings of the 60-Hz component. Also the distribution of the pulse magnitudes appear to be roughly Gaussian distributed. A Gaussian type distribution would not be expected for the nature of the mixed voltage waveform stressing the valve-winding insulation. These phenomena are likely cross-coupled

from discharges occurring at a location on the line-winding.

The C-phase valve-winding is characterized by three discharge phenomena on Fig. 4.15. The phenomena **(c1)** appears to be switching noise and resembles the phenomena **(a2)** that was observed on the A-phase valve-winding. The phenomena **(c2)** has a distinctly Gaussian or Weibull distribution and is therefore not likely native to the C-phase valve-winding. This phenomena **(c2)** is likely cross-coupled from the line-winding and appears to be the same phenomena as **(b2)** that was observed on the B-phase line-winding in Fig. 4.14. Lastly, the phenomena **(c3)** appears to be the same phenomena as **(a1)** that was observed from the A-phase valve-winding measurement. Cross-coupling here is likely because the valve-windings are delta-connected and there is an electrical connection between A and C-phase valve-windings. The analysis of the feature extracted data suggests that none of the discharge phenomena appearing in the C-phase valve-winding measurement are caused due to PD activity native to this winding.

4.4.3 Condition Assessment Analysis for On-line Measured Data

For the proper condition assessment of equipment having PD, it was expressed in Chapter 2 that trending and comparison of PD data acquired over time are a requirement. The magnitude of a PD pulse, acquired from a single measurement may be attenuated in propagation through the transformer before reaching the measurement sensors. Therefore pulse magnitude alone is not adequate to quantify

the severity of the discharge activity. In order to properly assess the degradation of the insulation, monitoring for changes in the magnitudes and repetition rate of a discharge phenomena must be observed over time. If the magnitudes and repetition rate of the discharge activity are increased significantly over time, only then can it be assessed that the insulation has been degraded to a point that it becomes a greater risk for failure.

Another essential requirement for the online PD measurement data is that the nature of the defect must be identifiable in order to have value for the condition assessment of the equipment. Without identification, the severity of the risk for failure cannot be established and thus there is no contribution to planning corrective maintenance. For example a PD phenomena identified in the winding paper insulation is of greater concern than discharges occurring in bubbles in oil.

In the online measurement data obtained from the HVDC converter transformer, there was one phenomena over the course of the monitoring period (July 20, 2007 to October 1, 2010) that was distinctly identifiable in the multiple acquisitions. This is the phenomena denoted as **(b1)** in Fig. 4.13 and Fig. 4.14. occurring on the B-phase line-winding. In Fig. 4.16, the history of periodic measurements that were performed on the B-phase line-winding show the progression of the phenomena **(b1)** aged over the three-year monitoring period.

The defect shown in Fig. 4.16, was diagnosed in Section 4.4.1, as a PD phenomena caused by corona discharges in oil from a point of high field stress. The

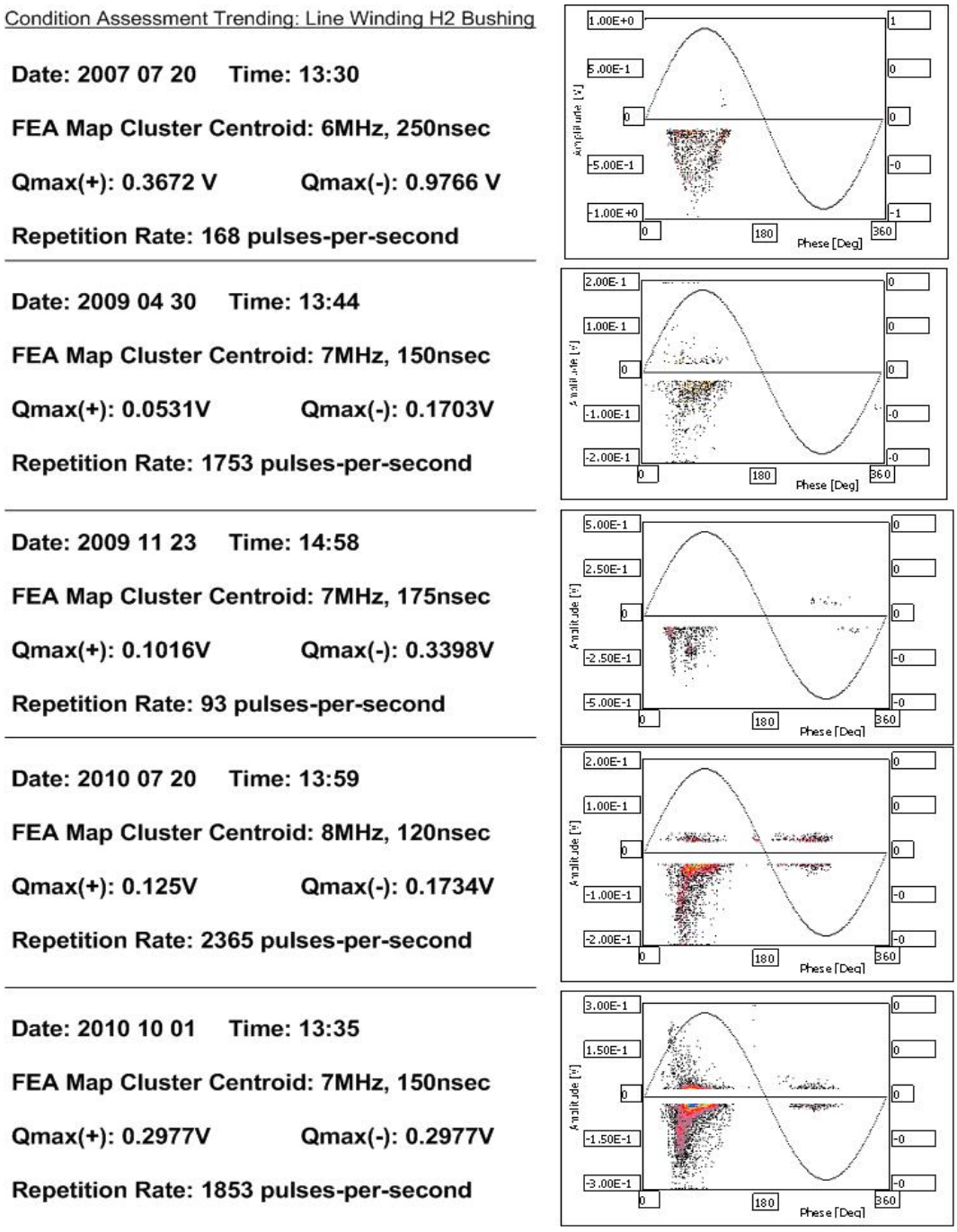

Fig. 4.16: Trended online PD measurements of a single phenomena between 2007 07 20 until 2010 10 01

defect does not appear to be degrading significantly with time because repetition rate and maximum discharge level do not appear to be increasing definitively over the period in which these measurements were made. The largest discharge activity for this phenomena was acquired on November 11, 2009. However, the repetition rate of the pulses in this acquisition were coincidently the lowest recorded during the monitoring period.

It is also noteworthy that on two separate monitoring sessions, performed on January 17, 2008 and October 10, 2008 the phenomena **(b1)** was absent from the measurement. It is possible that operating conditions were such that this PD phenomena did not occur at the time of the measurement. This suggests that the PD phenomena could be dependent upon conditions such as loading/temperature, or the tap position inside the transformer. Based on the small number of acquisitions performed in the three-year monitoring period, it is difficult to determine if these variables play a significant factor for the occurrence of the phenomena **(b1)**.

It is also possible that the phenomena was absent from the measurement for no reason associated to the operating conditions. In oil-paper insulation systems there is a potential for random appearance and disappearance of phenomena due to the dynamic nature of the insulating oil [24]. In Fig. 4.17, two acquisitions performed on the B-phase line-winding are performed two minutes apart. In the second acquisition, a discharge phenomena not previously present suddenly appears in the measurement. The control room was called to determine if there had been any

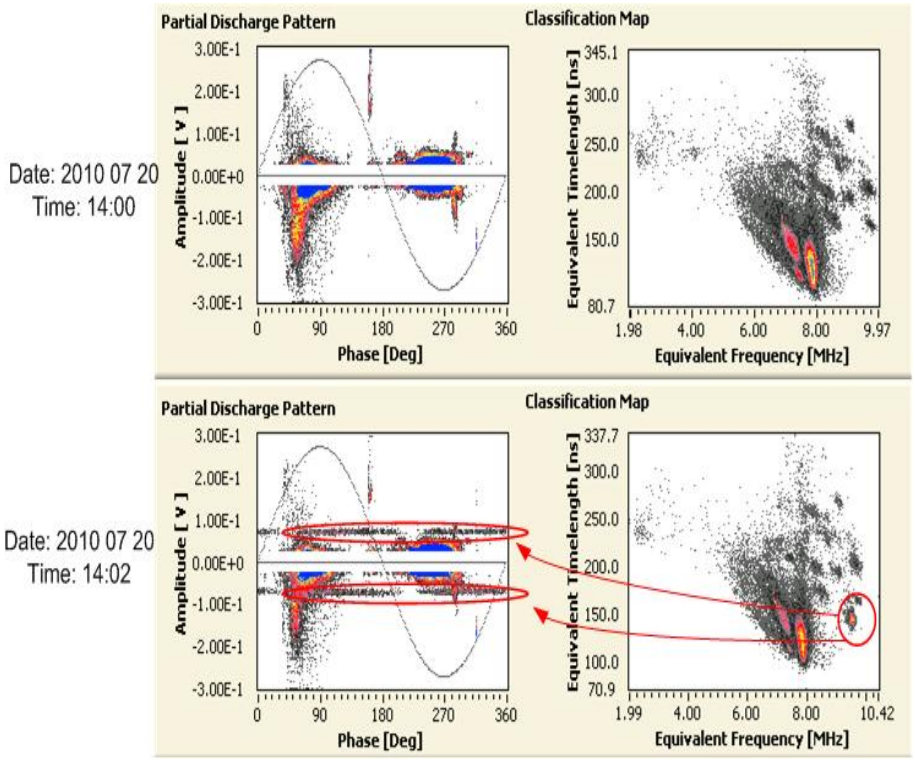

Fig. 4.17: Random appearance of PD phenomena with no changes to operating conditions.

changes to the operating conditions such as loading, voltage level, or tap changer position. The control room operator confirmed that there had not been any such changes. Therefore this phenomena appeared independently. It is speculated that inside the transformer tank, there exist gas bubbles suspended in the oil. When these gas bubbles move and out of high field stress regions within the insulation they can respectively cause PD phenomena to incept and extinguish. The oil movement through the transformer is circulated by both forced pumps, and natural convection processes.

This phenomena of appearance and disappearance, has implications for how on-

line PD measurements should be performed. Because phenomena can incept due to the circulation of oil, irrespective of the operating conditions, it becomes essential to increase the length of the acquisition. In this work, the acquisition intervals for PD measurement were anywhere between one and ten seconds. The results shown in Fig. 4.17 demonstrate that longer acquisition intervals are necessary. Based on what has been learned from this work, it is believed that an adequate acquisition interval is as long as one full-day in order to assess the transformer insulation by online PD measurement. With this length of acquisition duration the transformer insulation is exposed to a full loading cycle as well as a range of certain operating conditions that might incept an intermittent PD activity. Furthermore, it is advisable that measurements are performed in different seasons because different loading and temperature conditions may have an effect on the PD activity.

5. ONLINE PARTIAL DISCHARGE MONITORING OF AN HVDC CONVERTER WALL-BUSHING

In this chapter, the method and results of an online PD measurement, performed on HVDC wall bushings is described. The wall bushings of interest are located at the rectifier end and negative polarity pole of six pulse thyristor-controlled HVDC converter. These wall bushings are situated within the HVDC station as shown in Fig. 3.1. In service, the bushing insulation is stressed with the full pole direct voltage of -463.5kVdc.

The initial motivation behind performing these tests had arisen because chemical laboratory results found high concentrations of SF_6 decomposition byproducts in a gas sample taken from one of the wall bushings. The existence of these byproducts suggested that high levels of electrical discharge might be occurring within the bushing.

Prior to replacing the bushing, the opportunity was taken to perform online PD measurements. The defective bushing was located in the B-phase position of its converter group. Additionally, the C-phase bushing of this same group was monitored as a benchmark for comparison with the suspected faulty B-phase. A

successful recording of PD events from online measurements would provide valuable information for the identification of similar insulation defects in these wall bushings in the future.

5.1 Chemical Analysis of Gas Samples Taken from the Wall Bushings

As part of periodic offline maintenance, gas samples were taken in stainless steel cylinders from the wall bushings during scheduled outages for analysis by gas chromatography and Fourier transform infra-red spectroscopy at an external laboratory. The purpose of this analysis was to examine the integrity of the electrical insulation. These tests are capable of detecting trace amounts of decomposition byproducts in the gas. Relative concentrations of various SF_6 byproducts are indicative of particular defects.

A gas sample taken from the B-phase wall bushing showed high concentrations of known decomposition compounds. The most significant of these found, was sulfur deca-fluoride (S_2F_{10}). Sulfur deca-fluoride is a known decomposition byproduct of SF_6 resulting from electrical discharge activity [26]. Under normal conditions, no S_2F_{10} is present in SF_6. In the case of this bushing, approximately 0.5-percent of the total volume of the sample was S_2F_{10}, suggesting a serious electrical insulation defect.

5.2 Structure of the Bushing Insulation System and Description of Test Setup for Online PD Measurement

A schematic of the HVDC bushing and test setup is shown in Fig. 5.1. The interior structure of the bushing insulation system consists of two separate condenser cores that are joined by a gas duct at the wall of the valve hall. The condenser cores insulate the center conductor and grade the alternating voltage stress with respect to ground. The cores consist of resin-impregnated paper with embedded concentric aluminum foils. Each core terminates in a cone with the gas duct and this cone has a creepage distance of 431 mm.

A capacitance tap is connected to the second condenser foil of the outdoor core of the bushing. The capacitance tap provides a reference signal to the control room for voltage monitoring. It was not possible to disconnect this circuitry for the performance of the online PD measurements. The capacitance tap also serves as a means of making offline dielectric loss and capacitance measurements [4]. The capacitance tap has an approximate capacitance of 424 pF between itself and the high voltage conductor. It also has an approximate shunt capacitance from the tap to ground of 13,070 pF.

Unlike the capacitance tap, the test tap of the indoor core is connected to the first condenser foil of the indoor core of the wall bushing. In service, this tap is bonded to the bushing flange and wall.

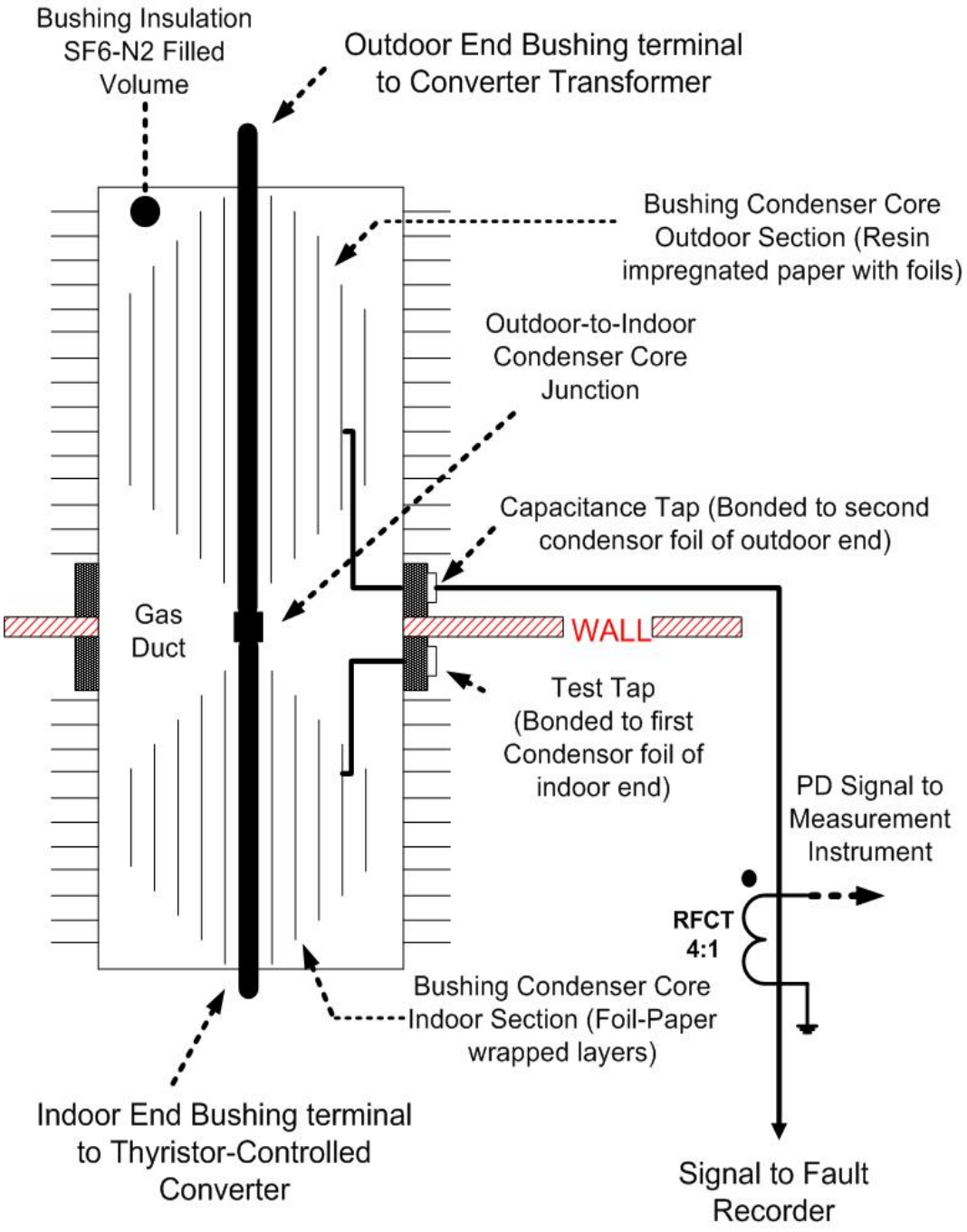

Fig. 5.1: HVDC Wall-bushing On-line PD measurement circuit

For the online measurement of PD, as was done for the transformer in the previous chapter, a high frequency current transformer was used to couple into the capacitance tap of the bushing to monitor the bushing insulation. What differs in the case of the bushing is that the measurement is directly coupled to the bushing insulation, whereas in the transformer case the insulation of the winding was monitored indirectly through the transformer bushing capacitance.

The PD measurement data was again recorded with the digital instrument called the *PDBase* manufactured by Techimp Systems. To remove some of the electromagnetic interference caused from the thyristor switching events, a 2.5-MHz high-pass filter was used at the input channel of the instrument.

One problem concerning the online measurement setup is that the bushing capacitance tap has a large capacitance to ground (C2=13 070 pF). For partial discharges which have very high frequency content, this large capacitance on the tap will have the effect of shunting some of the PD pulse currents to ground, and out of the measurement.

Another problem with the measurement setup is that a voltage reference was not available to provide a signal proportional to the actual voltage waveform stressing the bushing insulation. As mentioned in chapter 3, the voltage waveform stressing the bushing insulation is not sinusoidal, but mixed. It has an alternating voltage component, a large direct voltage component, and switching transient with harmonic components attributed to the HVDC conversion. The voltage waveform

stressing the bushing insulation is expected to be similar to that was shown in Fig. 3.3. As a result of not being able to capture this waveform directly during the online PD measurements, the PD events occurring could not be correlated with transient changes in the voltage stresses associated with the converter switching. Instead, for interpretation of this data, the PD pulse magnitudes were recorded on a phase-resolved plot. Where the reference source for the phase-resolved plot is synchronous with the alternating voltage component of the voltage stressing both bushing insulations.

5.3 Analysis of the Online Partial Discharge Measurement Data

The phase-resolved PD patterns acquired from the HVDC wall-bushings is shown in Fig. 5.2. The upper portion of the figure contains the phase-resolved PD plot and feature extraction map for the suspected faulty B-phase bushing. The lower row displays the same for the C-phase bushing.

For the analysis of the PD measurement data, a comparative method was used. Because the test specimens and setup for both bushings is identical, a comparison of PD measurement data on the phase-resolved plot is a suitable strategy for assessment. The phase-resolved plots are produced with respect to a source which is synchronous with the voltage stressing both bushings. On the phase-resolved plot, if pulses at a specific phase location appear larger in magnitude for one bushing than the other, then these pulses are likely to be PD occurring in the bushing

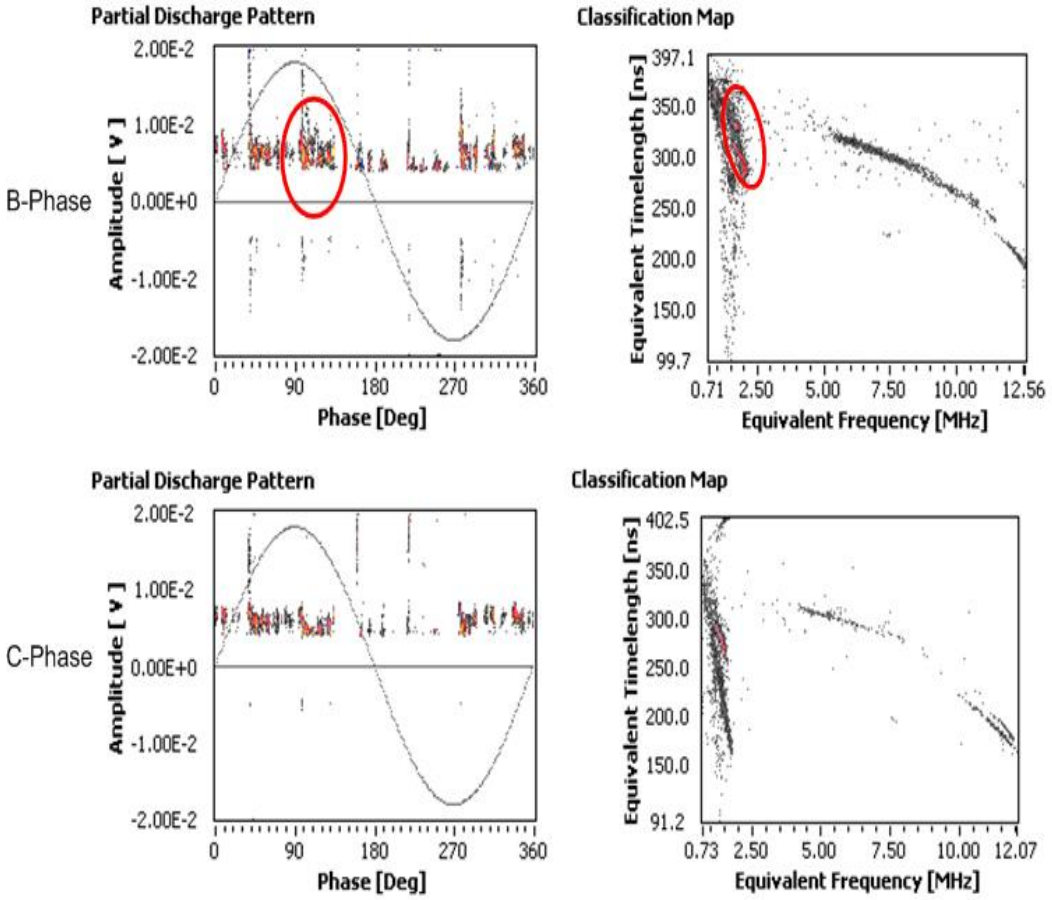

Fig. 5.2: Online PD Measurement Data. Top Row: B-phase (suspected faulty) Bushing Phase-Resolved Data and Classification Map, Bottom Row: C-phase Bushing Phase-Resolved PD and Classification Map

with larger magnitude pulses. This method of comparing relative magnitudes and assignment of a defect to the specimen with larger pulses is common and has been used in the development of other PD measurement instruments for online monitoring applications [27]. It appears that the thyristor firing in the HVDC conversion process has a significant influence on the discharges acquired through measurement. In the partial discharge pattern for B-phase there are six distinctive large discharge phenomena that occur synchronously over the 360-degree reference interval corresponding to the six-pulse converter operation.

At the phase location near 100-degrees there exists a succession of discharges following a switching pulse for the B-phase bushing. This phenomena is not present on C-phase. This can be seen more clearly when the phase-resolved plots for both the B and C-phase acquisitions are overlaid with one another as shown in Fig. 5.3. This suggests that the phenomena is native to the B-phase bushing.

Also the feature extraction map also shows a cluster of pulses centered at the map location of 2-MHz and 300 nanoseconds and is circled in red on Fig. 5.2. A similar cluster of pulses cannot be found in the C-phase acquisition. This suggests that there is a discharge phenomena, that is occurring only in the B-phase bushing. Using the feature extraction, this cluster of pulses and the resulting phase resolved PD pattern is isolated and shown in Fig. 5.4. These pulses have a peak maximum discharge voltage of approximately 10 millivolts and a repetition rate of approximately 930 pulses-per-second. The fact that these pulses are larger on

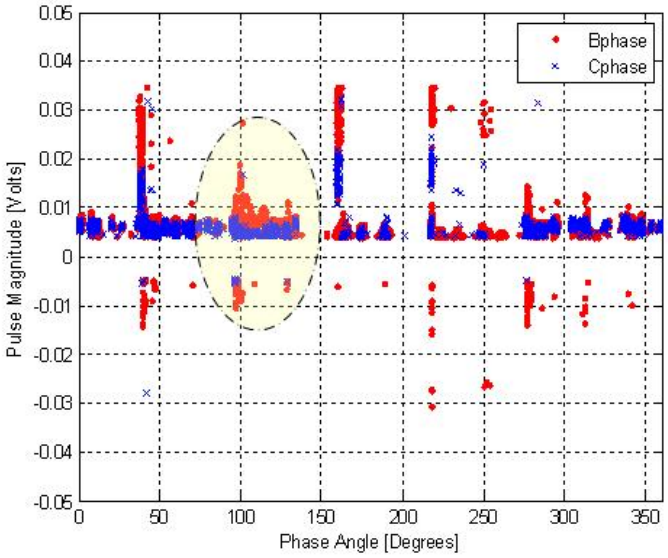

Fig. 5.3: Overlayed phase-resolved data for the B-phase and C-phase HVDC Bushings

the B-phase bushing than C-phase, along with the fact that the feature extraction method identified this phenomena as occurring only in B-phase, suggest that the phenomena is PD occurring in the B-phase bushing. It appears from the phase-resolved plots that discharges on the B-phase bushing may occur in response to a transient switching event on the B-phase converter. Furthermore, the fact that the discharge activity has predominantly positive polarity pulses is logical because this bushing is stressed with a large negative direct voltage offset. This also supports the asymmetry of the PD pattern because the voltage stress to the insulation is greater for the negative half-cycle of the 60-Hz component, than the positive.

This method of online PD measurement performed on HVDC converter bushings shows promise in its ability to isolate PD phenomena for interpretation. The

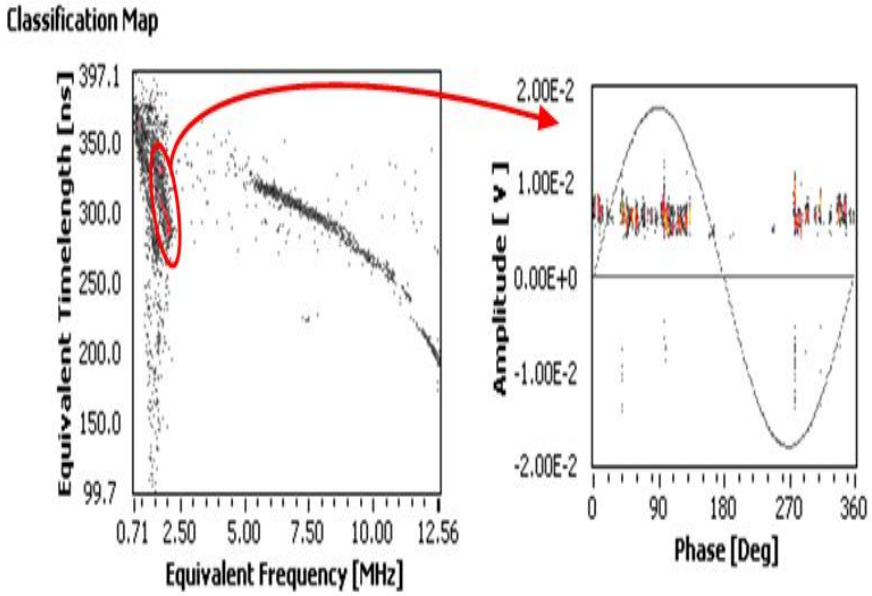

Fig. 5.4: Feature Extraction Isolation of suspected PDs occurring in the B phase bushing

isolation of this cluster of pulses through feature extraction, enables condition assessment. In the case of the B-phase bushing the discharge phenomena characterized by the cluster of pulses located at 2 MHz, and 300 nano-seconds on the feature extraction map, could be isolated and trended over time. If the magnitude of the pulses, or their repetition rate increase over time, then it could be determined that the condition of the insulation is degraded.

It is important to note that without the acquisition of data from the C-phase bushing for a baseline comparison, the identification of PD on the B-phase bushing would have been much more difficult. If the phase-resolved plot and feature extraction map were available for the B-phase bushing alone, discerning what discharge phenomena were PD from what were switching noise becomes almost impossible

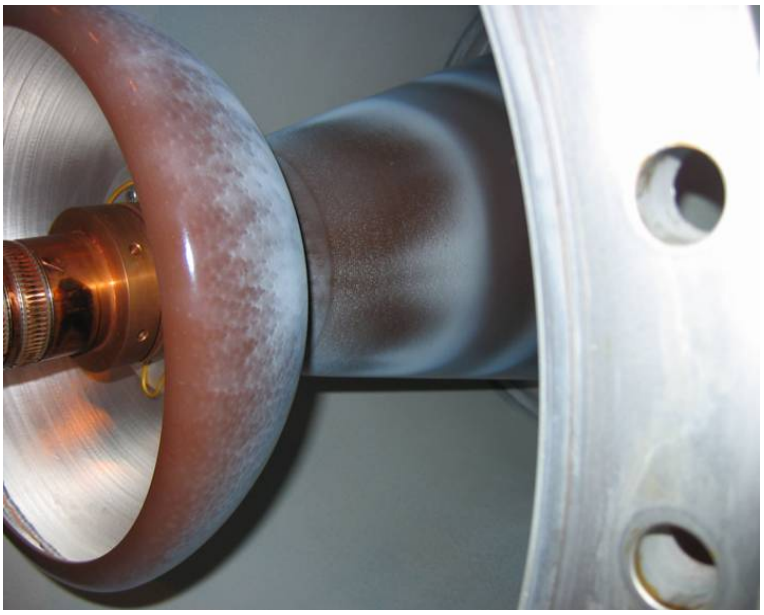

Fig. 5.5: Physical evidenc of PD found in the B-phase wall bushing

to interpret. As a result, the comparative method of measurement is considered a much better method of analysis for equipment subjected to mixed HVDC voltage stress.

5.4 Resultant Findings for Physical Evidence of Partial Discharges

After the B-phase bushing was removed from service, physical evidence of PD was found. A chalky white deposit was discovered on the stress cone of the bushing condenser core near the joint between on the outdoor sections as shown in Fig. 5.5. This deposit was caused from the chemical byproducts of PD occurring in the SF_6 gas. These findings support the online PD measurements which suggested PD activity was occurring in the B-phase wall bushing.

6. CONCLUSIONS AND FUTURE WORK

This work has shown that the performance of online PD measurements in a high noise station environment are feasible. The most significant contribution of this work has been the development of techniques required for the performance and analysis of online PD measurements of HVDC apparatus. The work has validated modern signal processing methods for feature extraction and their ability to aid in the removal of noise from measurement, as well as isolate multiple PD phenomena occurring simultaneously in high-voltage equipment. It has been demonstrated that the isolation of PD phenomena enables trending, which is essential for online PD measurement to provide value as a condition assessment tool.

The are a number of key findings from this research. The characterization of the mixed voltage stresses imposed on HVDC equipment identified that PD may occur in response to direct, alternating, and/or switching transient components. From the online PD measurements performed, discharge phenomena were attributed to each of these stresses.

The HVDC station noise environment was characterized as having significant switching noise in the bandwidth region around 1.5-MHz. As a result it was

discovered that the negative impact of electromagnetic interference (noise) in PD measurement could be mitigated by a combination of high-pass filtering and signal processing methods for feature extraction.

The so-called method of moments feature extraction method was analyzed in depth. The algorithm was reproduced in MATLAB and applied to pulse waveform data in order to observe the effects of propagation distortion on feature extraction. A relationship between propagation distortion and the feature extraction map was discovered. This relationship was further used in the interpretation of online PD measurement data.

Additionally this work has enhanced the knowledge for how these online measurements should be performed. For oil-paper insulation systems such as power transformers, it has been learned that longer acquisition durations are necessary for the PD measurement. Oil-paper insulation, has unique qualities which allow for the appearance and disappearance of phenomena irrespective of the operating conditions of the apparatus. Increasing the duration of the acquisition increases the chances of capturing certain PD phenomena.

For insulation under mixed voltage stresses, associated with the HVDC conversion process, interpretation and identification are more difficult. Value obtained from the measurement becomes more dependent on long-term trending of the PD data. When possible, comparative methods of online PD measurement are better suited for these applications. This has been shown from the successful application

of a comparative method of PD measurement on HVDC converter wall bushings in this thesis.

In future work, the development and/or evaluation of other feature extraction techniques could be of value. It is believed that through the acquisition of more online PD measurement data, that the interpretation of measurements performed under mixed voltage stress will improve. However, for large apparatus PD measurement is by nature constrained by issues relating to measurement sensitivity. The real value of online PD measurement may be realized in its correlation and integration with other insulation diagnostic techniques. In other future work, online PD measurement could be correlated with other online diagnostics such as oil and gas-analysis testing [28].

REFERENCES

[1] N. C. Sahoo, M. M. A. Salama, and R. Bartnikas, "Trends in partial discharge classification: A survey," *IEEE Trans. on Dielectrics and Electrical Insulation*, vol. 12, no. 2, pp. 248–264, April 2005.

[2] W. McDermid, A. Glodjo, and J. C. Bromley, "Analysis of winding failures in hvdc converter transformers," in *Proc. 1999 Electrical Insulation Conf. and Electrical Manufacturing and Coil Winding Conference*, Cincinnati, OH, USA, October 26-October 28 1999, pp. 653–657.

[3] *IEC 60270 High-Voltage Test Techniques-Partial Discharge Measurements 2000*, 2000.

[4] E. Kuffel, W. S. Zaengl, and J. Kuffel, *High Voltage Engineering Fundamentals 2nd Edition*. Elsevier Ltd., 2000.

[5] R. Bartnikas, "Corona discharge processes in voids," *Engineering Dielectrics Vol.1 - Corona measurement and interpretation, ASTM STP669*, vol. 1, no. 1, pp. 22–67, February 1979.

[6] R. J. Densley, "Partial discharges under direct-voltage conditions," *Engineering Dielectrics Vol.1 - Corona measurement and interpretation, ASTM STP669*, vol. 1, no. 1, pp. 409–463, 1979.

[7] I. W. McAllister, "Electric field theory and the fallacy of void capacitance," *IEEE Trans. on Electrical Insulation*, vol. 26, no. 3, pp. 458–459, June 1991.

[8] Z. Achillides, G. E. Georghiou, and E. Kyriakides, "Partial discharges and associated transients: The induced charge concept versus capacitive modeling," *IEEE Trans. on Dielectrics and Electrical Insulation*, vol. 15, no. 6, pp. 1507–1516, December 2008.

[9] M. Fenger, S. R. Campbell, and J. Pederson, "Dealing with motor winding problems caused by inverter drives," in *Proc. 2002 Cement Industry Technical Conference*. Jacksonville, USA: IEEE, May 2002, pp. 65–76.

[10] *IEEE Standard 62 Guide for Diagnostic Field Testing of Electric Power Apparatus-Part 1: Oil Filled Power Transformers, Regulators and Reactors*, 1995.

[11] M. Cacciai, A. Contin, G. Rabach, and G. C. Montanari, "An approach to partial discharge investigation by height distribution analysis," *IEE Proceedings on Science Measurement and Technology*, vol. 142, no. 1, pp. 102–108, January 1995.

[12] A. Contin, A. Cavallini, and C. Ferraro, "Pd source recognition by weibull processing of pulse height distributions," *IEEE Trans. on Dielectrics and Electrical Insulation*, vol. 7, no. 1, pp. 48–58, February 2000.

[13] B. Fruth and L. Niemeyer, "The importance of statistical characteristics of partial discharge data," *IEEE Trans. on Dielectrics and Electrical Insulation*, vol. 27, no. 1, pp. 60–69, February 1992.

[14] D. A. Nattrass, "Partial discharge measurement and interpretation," *IEEE Electrical Insulation Magazine*, vol. 4, no. 3, pp. 10–28, 1988.

[15] P. H. F. Morshuis and J. J. Smit, "Partial discharges at dc voltage: Their mechanism detection and analysis," *IEEE Trans. on Dielectrics and Electrical Insulation*, vol. 12, no. 2, pp. 328–340, April 2005.

[16] S. Wenrong, L. Junhao, Y. Peng, and L. Yanming, "Digital detection grouping and classification of partial discharge signals at dc voltage," *IEEE Trans. on Dielectrics and Electrical Insulation*, vol. 15, no. 6, pp. 1663–1674, December 2008.

[17] T. Babnik, R. K. Aggarwal, and P. J. Moore, "Principal component hierarchiacal cluster analyses as applied to transformer partial discharge data with particular reference to transformer condition monitoring," *IEEE Trans. on Power Delivery*, vol. 23, no. 3, pp. 2008–2016, October 2008.

[18] A. Contin, A. Cavallini, G. C. Montanari, G. Pasini, and F. Puletti, "Digital detection and fuzzy classification of partial discharge signals," *IEEE Trans. on Dielectrics and Electrical Insulation*, vol. 9, no. 3, pp. 335–348, June 2002.

[19] I. Gath and A. B. Geva, "Unsupervised optimal fuzzy clustering," *IEEE Trans. on Pattern Analysis and Machine Intelligence*, vol. 11, no. 7, pp. 773–781, July 1989.

[20] D. W. Hard, *Introduction to Power Electronics.* Upper Saddle River NJ: Prentice Hall, 1997.

[21] A. Cavallini, G. C. Montanari, F. Puletti, and A. Contin, "A new methodology for the identification of pd in electrical apparatus: Properties and applications," *IEEE Trans. on Dielectrics and Electrical Insulation*, vol. 12, no. 7, pp. 203–215, April 2005.

[22] N. D. Jacob, W. M. McDermid, and B. Kordi, "Partial discharge propagation distortion and implications for feature extraction methods in online monitoring," in *Proc. 2010 International Symposium on Electrical Insulation*. San Diego, USA: IEEE, 2010, pp. 429–432.

[23] Q. Shaozhen and S. Birlasekaran, "The study of propagation characteristics of partial discharge in transformers," in *Proc. 2002 Conference on Electrical Insulation and Dielectric Phenomena*, Cancun, Mexico, 2002, pp. 446–449.

[24] A. Cavallini, G. C. Montanari, and F. Ciani, "Analysis of partial discharge in paper-oil insulation systems as a basis for risk assessment evaluation," in *International Conference on Dielectric Liquids*. Coimbra, Portugal: IEEE, 2005, pp. 241–244.

[25] S. M. Strachan, S. Rudd, S. D. McArthur, M. D. Judd, S. Meijer, and E. Gulski, "Knowledge based diagnosis of partial discharges in power transformers," *IEEE Trans. on Dielectrics and Electrical Insulation*, vol. 15, no. 1, pp. 259–268, February 2008.

[26] H. D. Morrison, V. P. Cronin, F. Y. Chu, M. Eygenraam, I. Sauers, and M. J. Dallavalli, *Gaseous Dielectrics VII*. Plenum Press, 1994.

[27] Z. Berler, A. Golubev, A. Romashkov, and I. Blokhinstev, "A new method of partial discharge measurements," in *Proc. 1998 Electrical Insulation and Dielectric Phenomena*. Atlanta, GA: IEEE, 1998, pp. 315–318.

[28] M. Horning, J. Kelly, S. Meyers, and R. Stebbins, *Transformer Maintenance Guide 3rd Edition*. S. D. Meyers, 2004.